Chapter 5
Fine Mass Concentrations

This chapter presents an analysis of the CASTNet visibility-related air quality measurements, i.e., fine particle mass ($PM_{2.5}$) and its estimated chemical constituents. Measurements taken in 1999 are emphasized, although data from 1994 through 1999 are presented and discussed. Annual, quarterly, and peak 24-hour concentrations and their chemical constituents for the 6-year period are shown. Relationships between $PM_{2.5}$ and SO_4^{2-} concentrations are also presented.

The entire visibility database was subjected to a new validation criterion based on flow volume. Twenty-four hour flow had to range between 75 and 125 percent of the expected value in order for the concentrations to be considered valid. If the flow values fell outside this range, the concentrations were invalidated. The analyses and figures presented in this chapter are based on the new database. The new validation criterion resulted in the invalidation of two quarterly averages. To complete the figures with time series, the invalidated (missing) quarterly values were interpolated from adjacent values

Figure 5-1 presents 1999 annual and quarterly averages of $PM_{2.5}$ concentrations measured at the eight visibility sites. Peak 24-hour concentrations measured during each quarter and for the year are plotted adjacent to the annual/seasonal averages. During 1999, the highest seasonal and 24-hour averages were generally observed during the third quarter. Annual values measured in 1999 at all eight sites are below 15 $\mu g/m^3$ and 24-hour values are below 65 $\mu g/m^3$.

Figure 5-2 presents a map of annual averages of reconstructed fine mass. The data are displayed in the form of a pie chart for each of the eight sites. The numerical value outside the pie is the corresponding measured $PM_{2.5}$ concentration. The fine mass was reconstructed using the parameters recommended by Sisler *et al.* (1996) and discussed in more detail for CASTNet by Lavery and Howell (2000). Sulfate (as ammonium sulfate) is the major contributor to fine mass at seven of the eight sites. Organic carbon and nitrate are also important contributors. Organic carbon was the primary constituent at the Sikes, LA (SIK570) site during 1999. Figures 5-3 through 5-6 are maps of pie charts of

1999 quarterly reconstructed fine mass. The highest quarterly averages were measured during the third quarter at all but two sites – Arendtsville, PA (ARE528) and SIK570. SO_4^{2-} concentrations also peaked in the third quarter. Organic carbon is a large component, especially in the warmer seasons and regions of the country. NO_3^- is relatively important at sites in colder climates and during the colder quarters (e.g., see Figure 5-3). The latter is consistent with the geographic and seasonal distribution of NO_3^- measured in the dry deposition network (Appendix C).

Figures 5-7 through 5-14 present time series of quarterly values of measured $PM_{2.5}$ and their reconstructed chemical constituents for each CASTNet site over the period fourth quarter 1993 through fourth quarter 1999. The figures are sequenced beginning in the northeast and moving to the southwest, i.e., from Connecticut Hill, NY (CTH510) to SIK570. The legend on the figures explains the different shadings. The measured $PM_{2.5}$ concentration is given by the diamonds. Two values for the second quarter 1995 (Figures 5-12 and 5-14) were interpolated from adjacent quarterly values. The time series for the eight sites are fairly similar in that quarterly $PM_{2.5}$ values follow the annual cycle of SO_4^{2-}, which peaks in the summer months. However, the relative contributions of organic carbon and NO_3^- are variable from site to site and season to season. SIK570 continues to measure low nitrate, relatively high carbon, and some soil dust. No trend is evident in the quarterly concentrations.

Bar charts that illustrate annual average and peak 24-hour concentrations of $PM_{2.5}$ and its constituents are shown in Figures 5-15 through 5-22. Annual values are not presented for 1996 because of the network shutdown. Sulfate contributes approximately half of the mass at the three western most sites and a larger fraction at the other five sites. Table 5-1 summarizes the highest annual values for the eight sites, independent of year.

The peak 24-hour values that are presented are based on the availability of both measured $PM_{2.5}$ and reconstructed mass for those 24-hour periods. The peak 24-hour concentrations were selected based on the peak $PM_{2.5}$ values for each year. The highest 24-hour concentrations range from about 25 to 69 $\mu g/m^3$. The highest concentrations are usually observed in the third quarter when sulfate values are at their maximum. Two exceptions occurred in 1999. The highest value at ARE528 was measured in the first quarter. Sulfate, nitrate, and organic carbon all contributed significantly. The highest value at SIK570 was observed during the fourth quarter. This peak value was produced by an unusual occurrence of organic carbon, which contributed approximately 85% of the mass. Table 5-2 summarizes the highest 24-hour concentrations measured by each of the eight sites during the entire operation of the network.

Annual averages of $PM_{2.5}$ mass, sulfate, nitrate, and organic carbon concentrations were aggregated over the eight visibility sites. Values for 1996 were interpolated from adjacent years. Aggregated annual averages are plotted in Figure 5-23. Linear regressions were fit through the four sets of annual averages. The results indicate no trends in annual averages. Box plots for $PM_{2.5}$, ammonium sulfate, ammonium nitrate, and organic carbon are given in Figures 5-24 through 5-27.

Scattergrams of 24-hour $PM_{2.5}$ and SO_4^{2-} concentrations measured at all eight visibility sites together are given in Figures 5-28(a) and (b) for the four quarters of 1999. The four scatter plots show reasonable correlation, indicating a relationship between fine mass and sulfate throughout the year. These scatter plots and the previous analyses demonstrate clearly that sulfate is a major contributor to atmospheric fine mass loading.

Figure 5-1. Annual and Quarterly Average/Peak 24-hour Concentrations (µg/m^3) of Fine Particle Mass for 1999

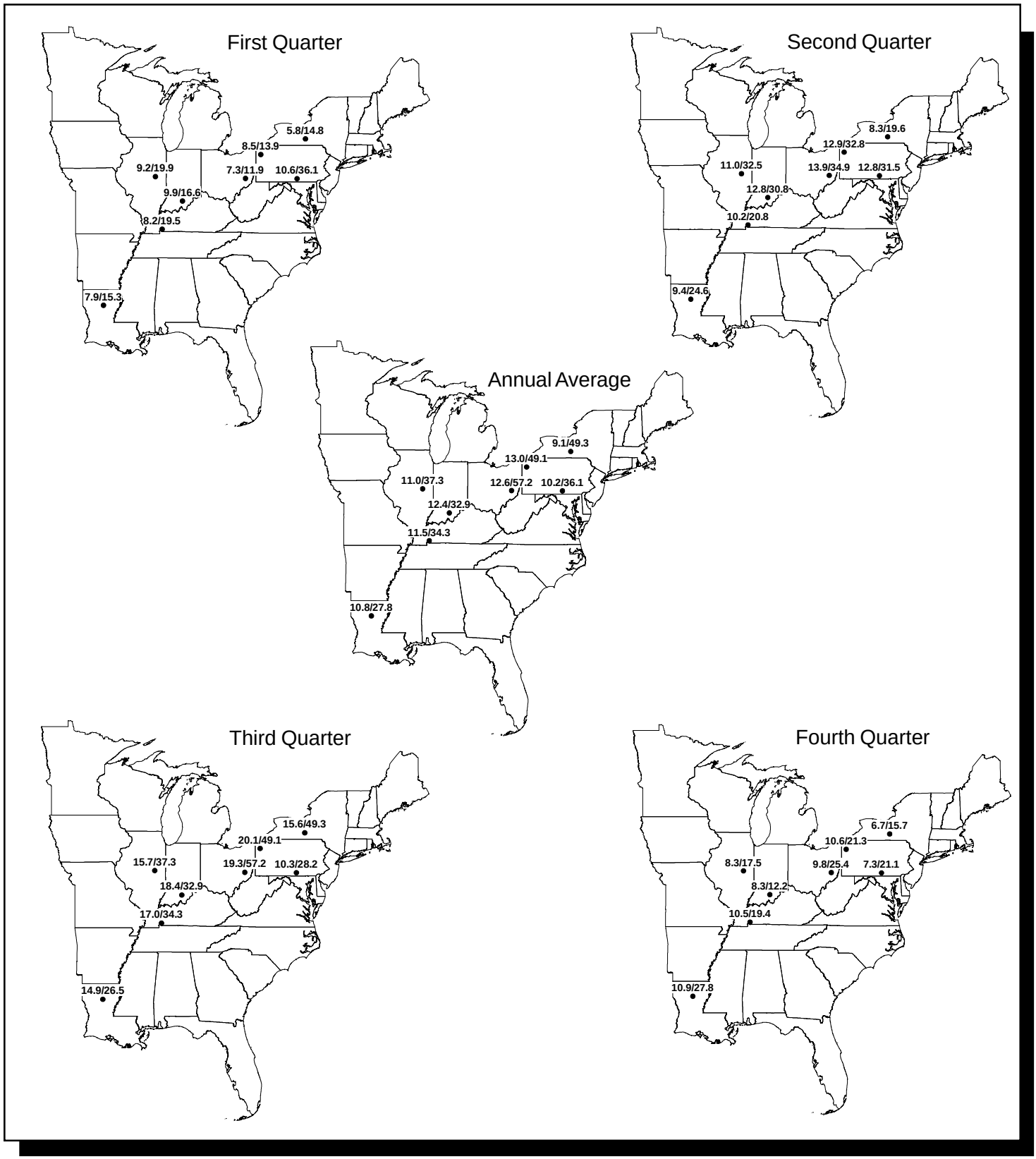

Figure 5-2. 1999 Annual Reconstructed Fine Mass

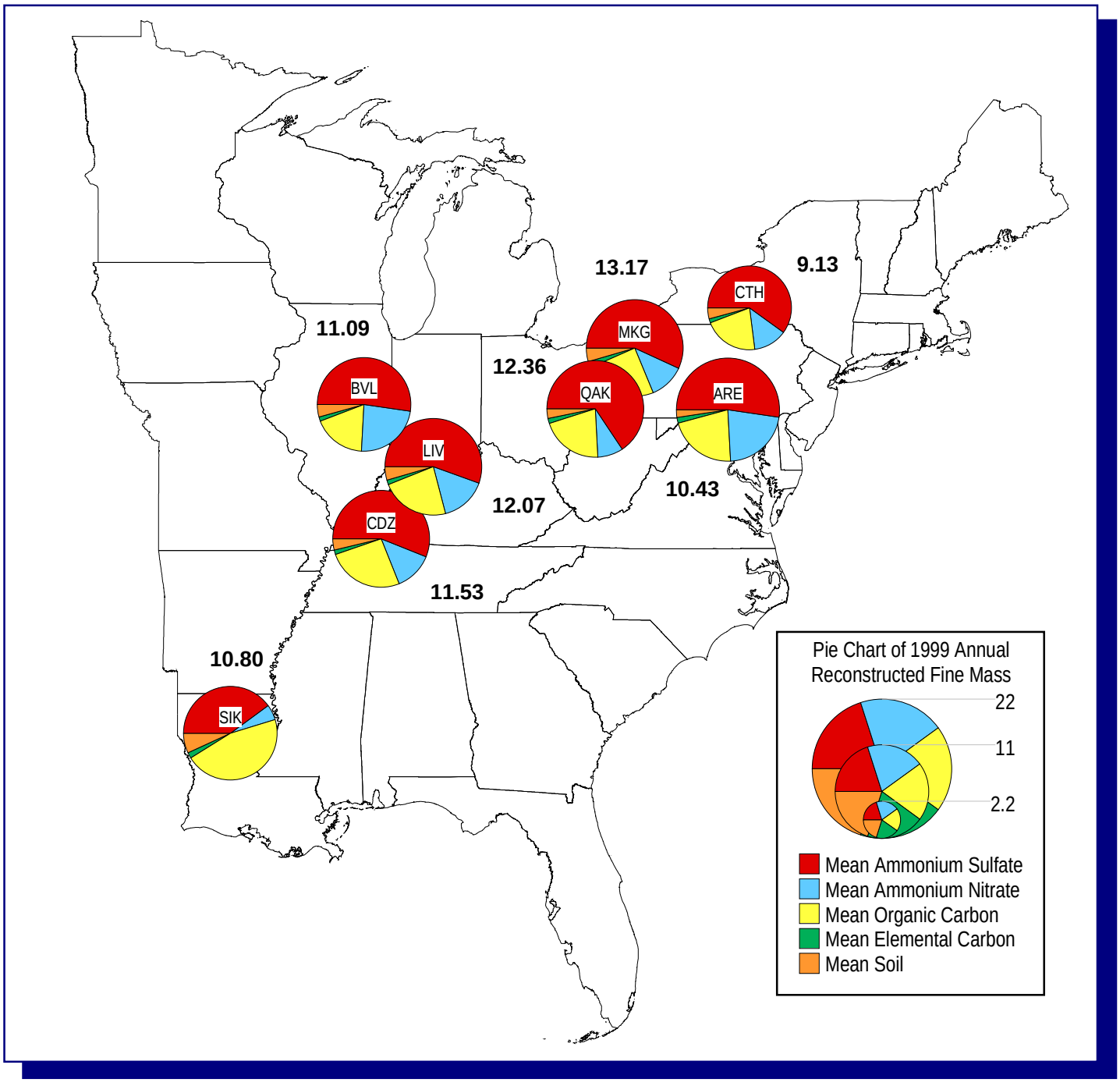

Figure 5-3. First Quarter 1999 Reconstructed Fine Mass

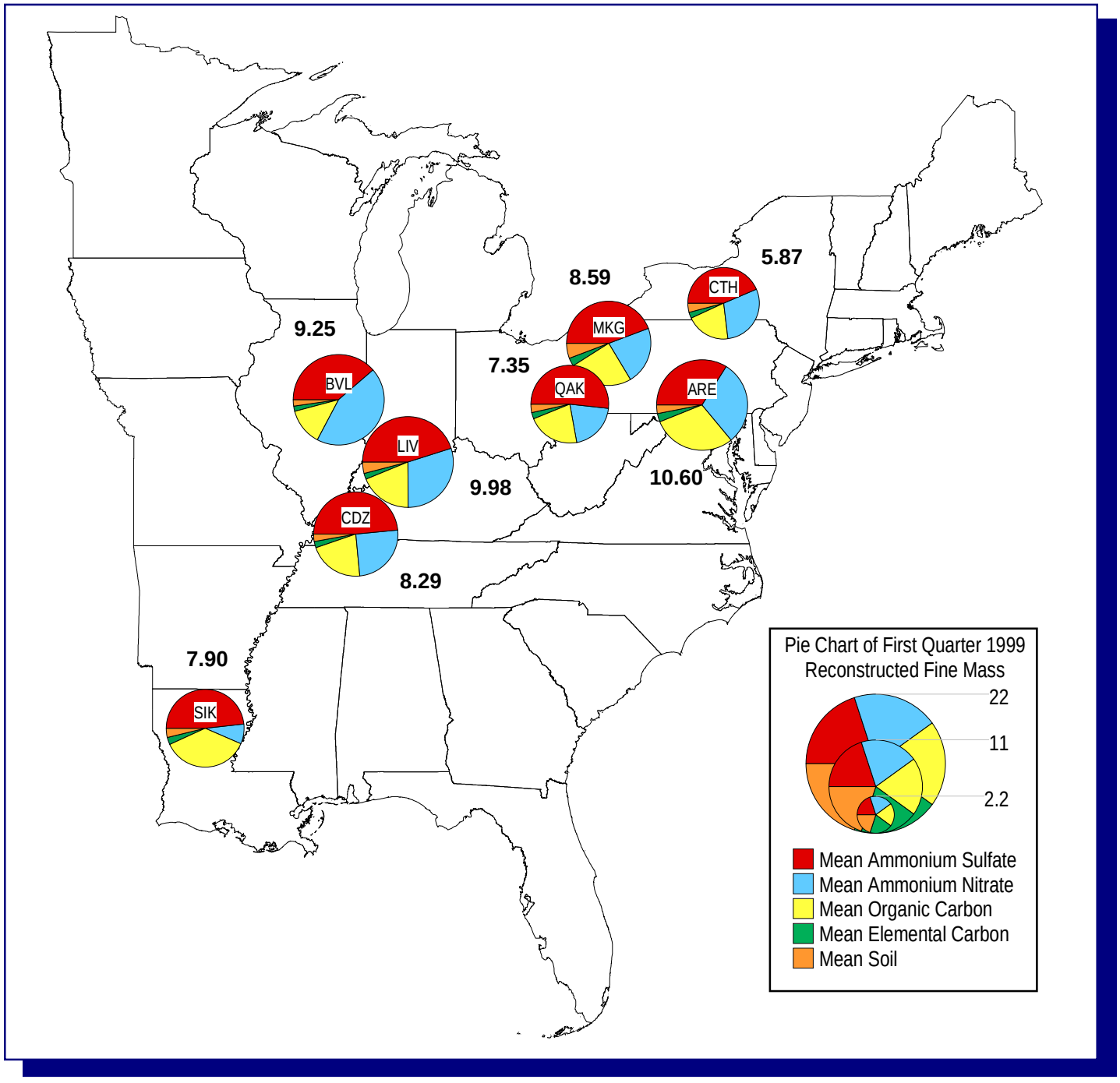

Figure 5-4. Second Quarter 1999 Reconstructed Fine Mass

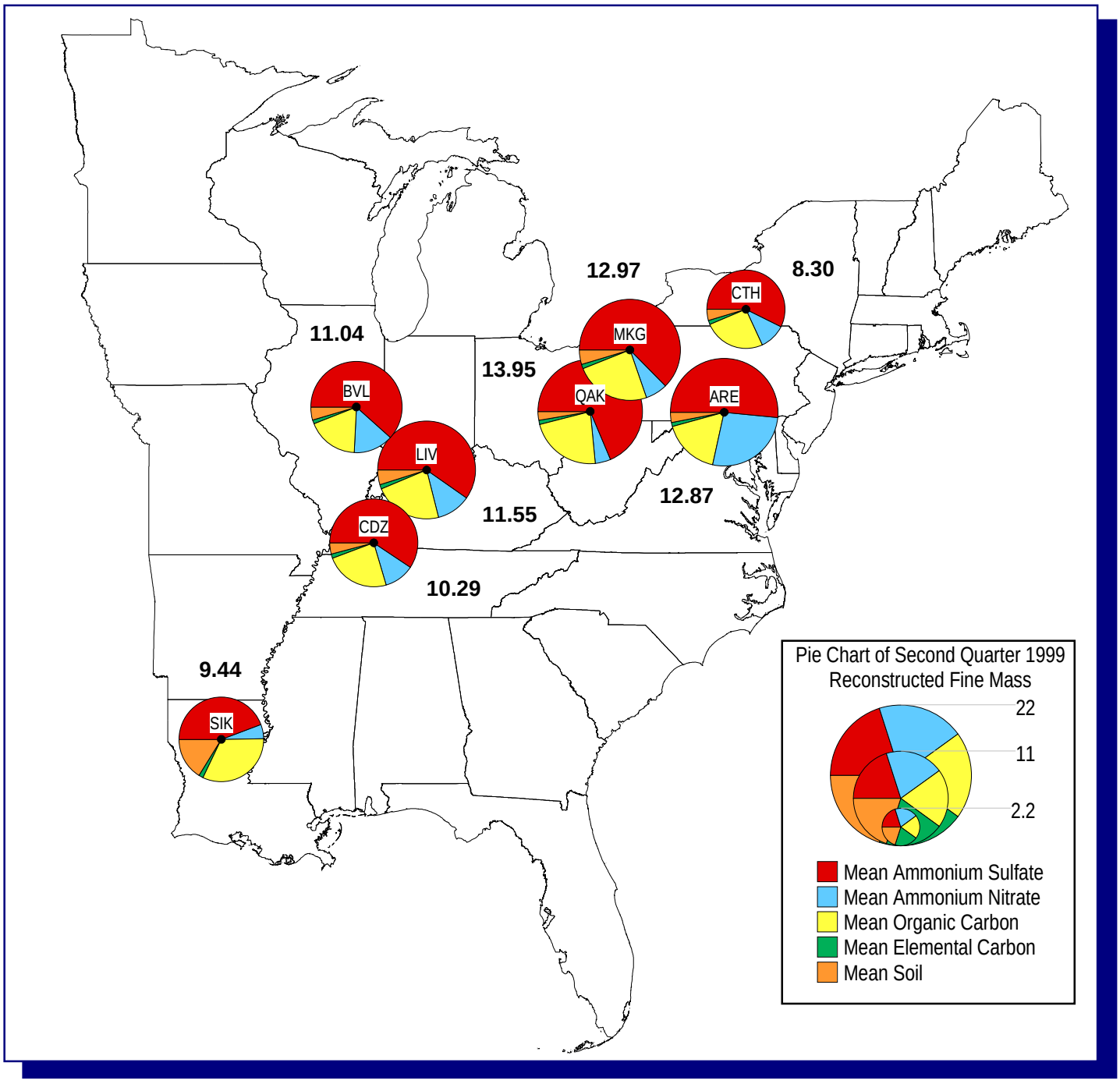

Figure 5-5. Third Quarter 1999 Reconstructed Fine Mass

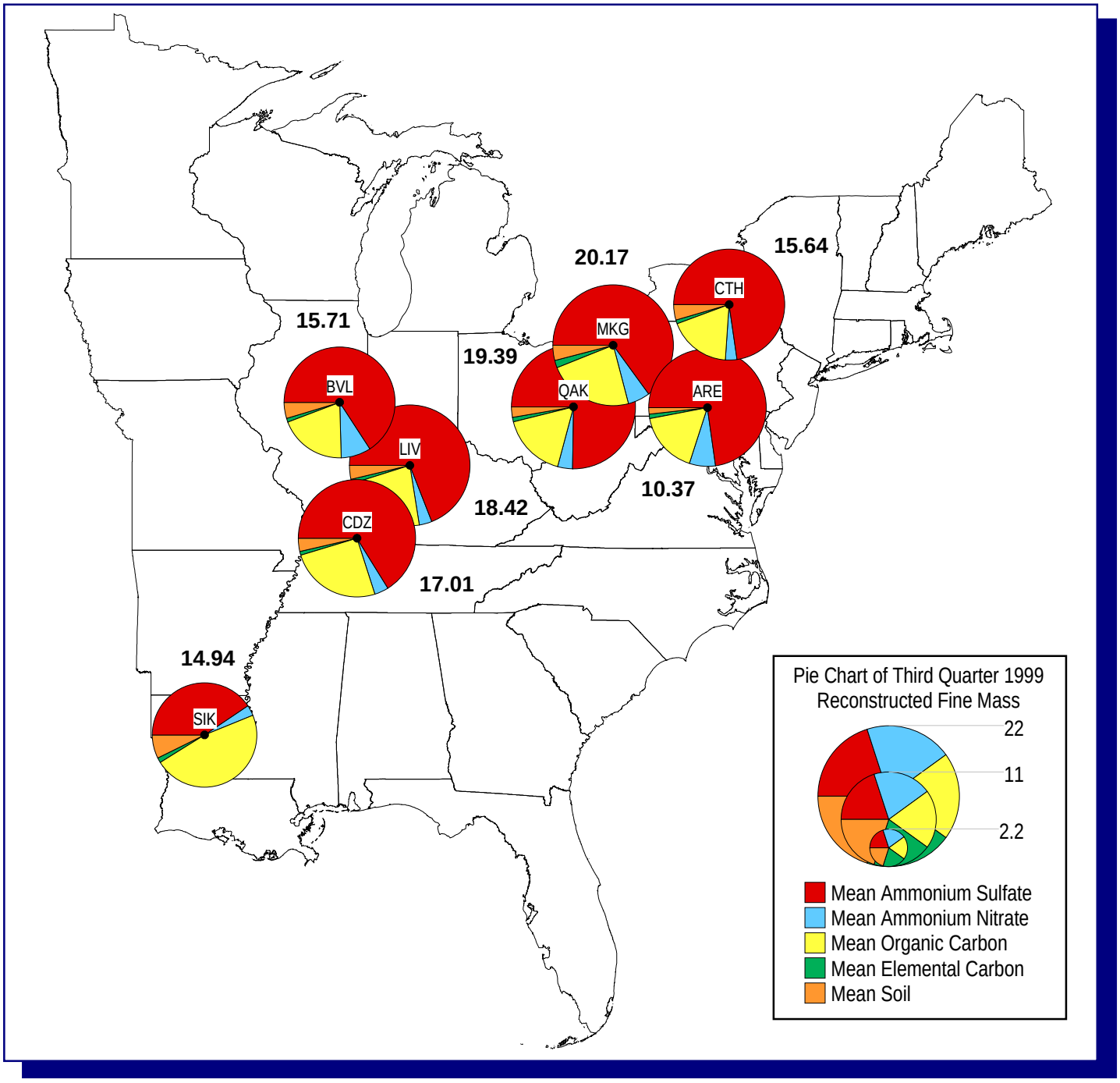

Figure 5-6. Fourth Quarter 1999 Reconstructed Fine Mass

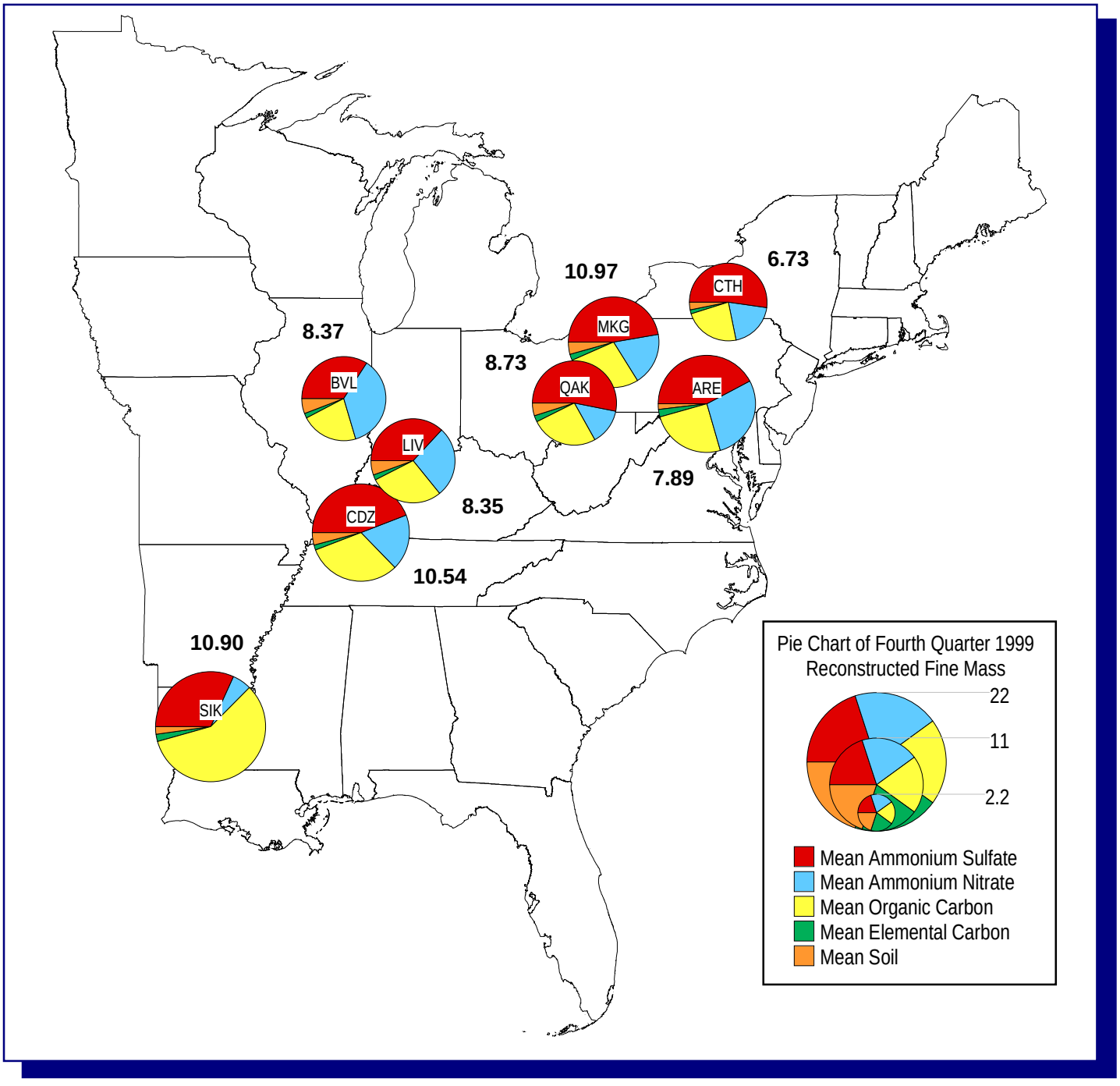

This page intentionally left blank.

Figure 5-7. Time Series of Quarterly Reconstructed Fine Mass at Site CTH510

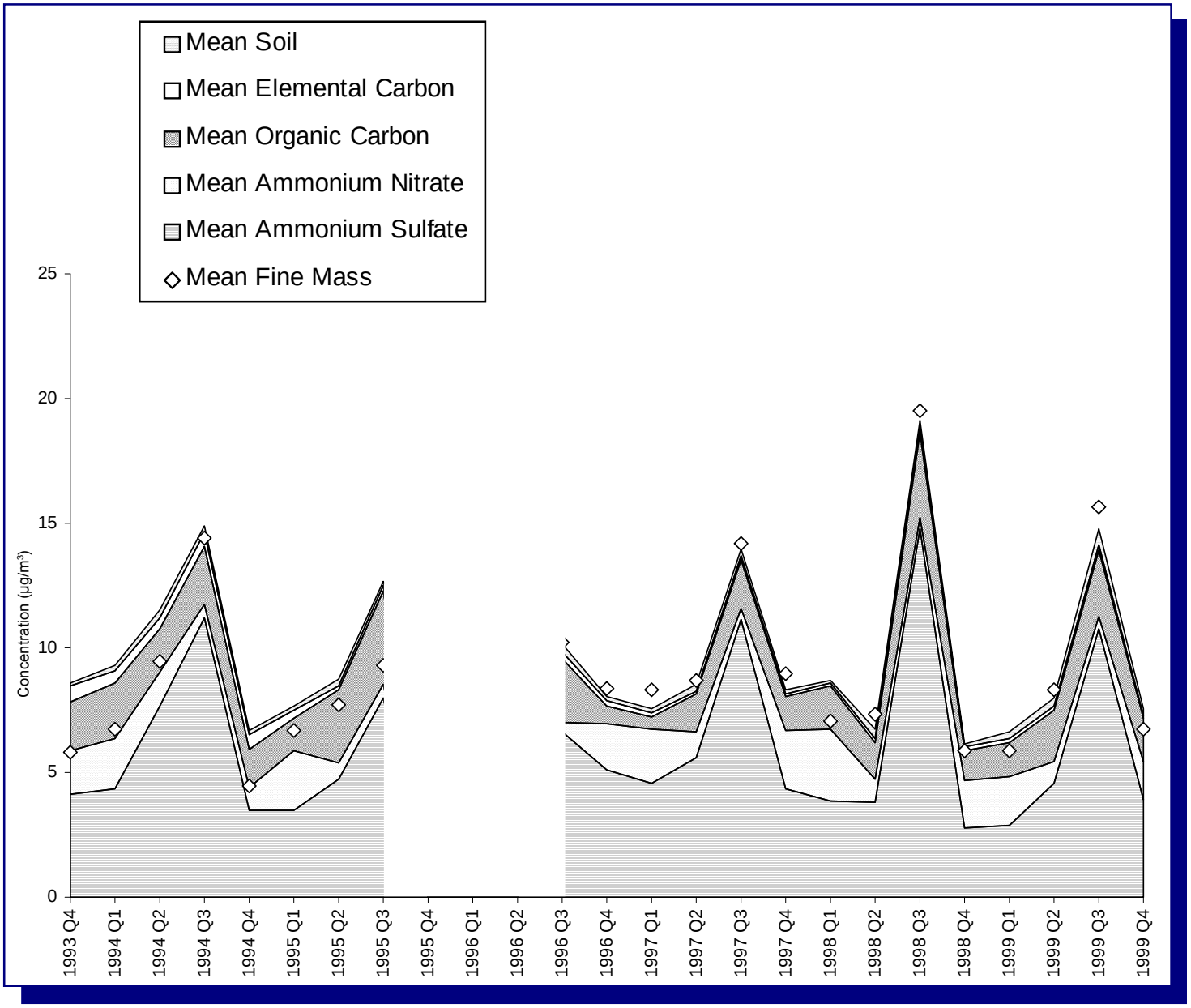

Figure 5-8. Time Series of Quarterly Reconstructed Fine Mass at Site ARE528

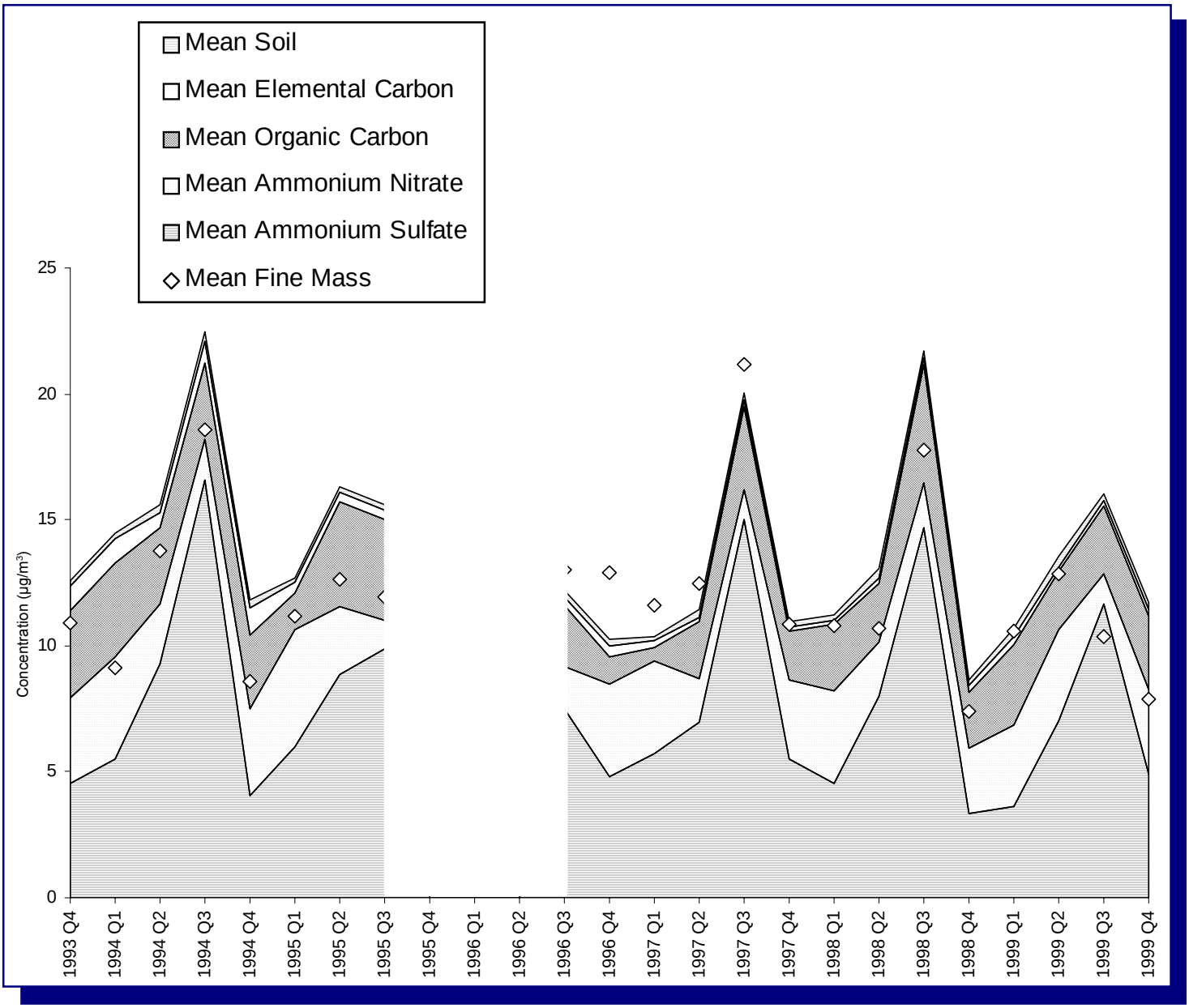

Figure 5-9. Time Series of Quarterly Reconstructed Fine Mass at Site MKG513

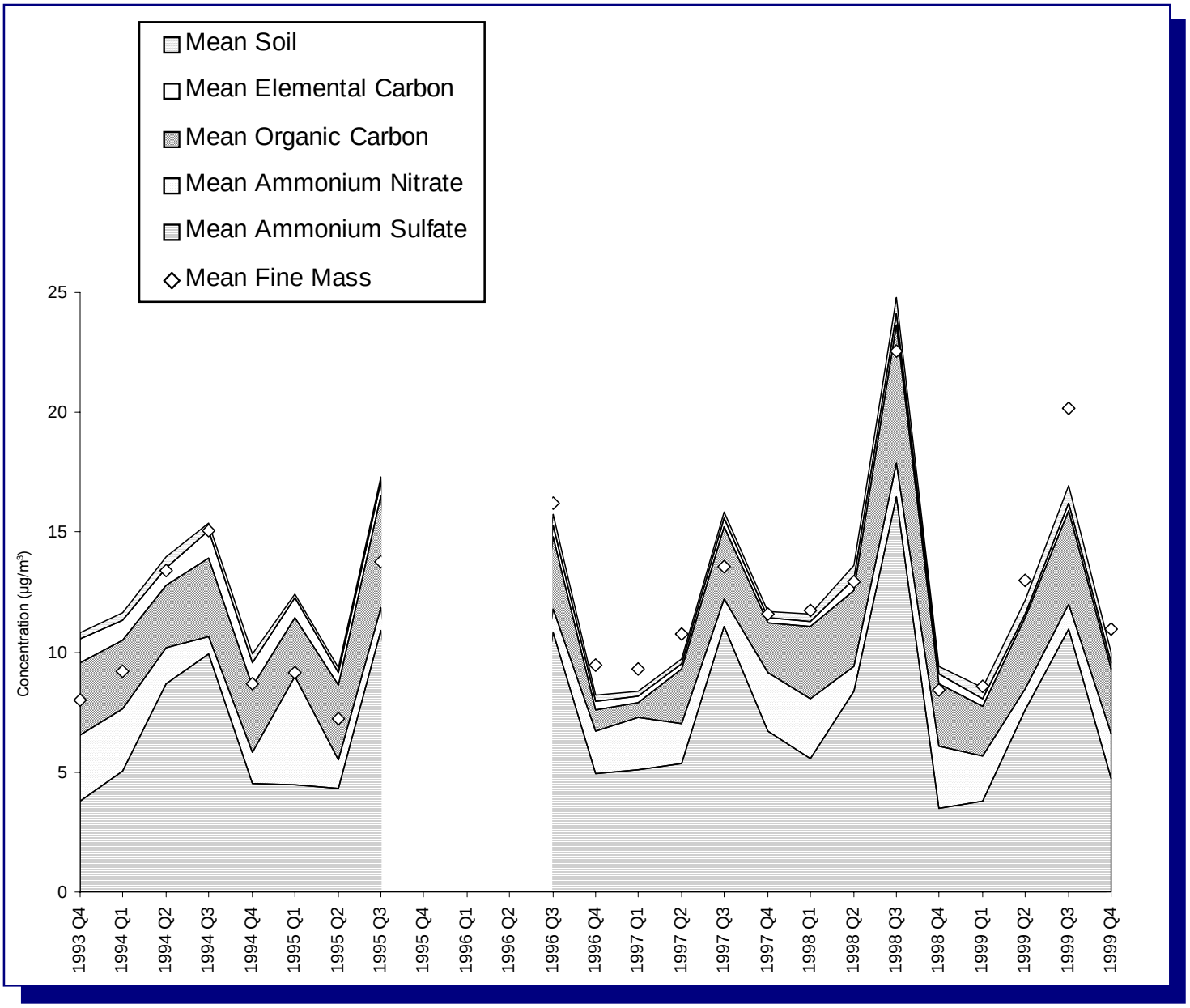

Figure 5-10. Time Series of Quarterly Reconstructed Fine Mass at Site QAK572

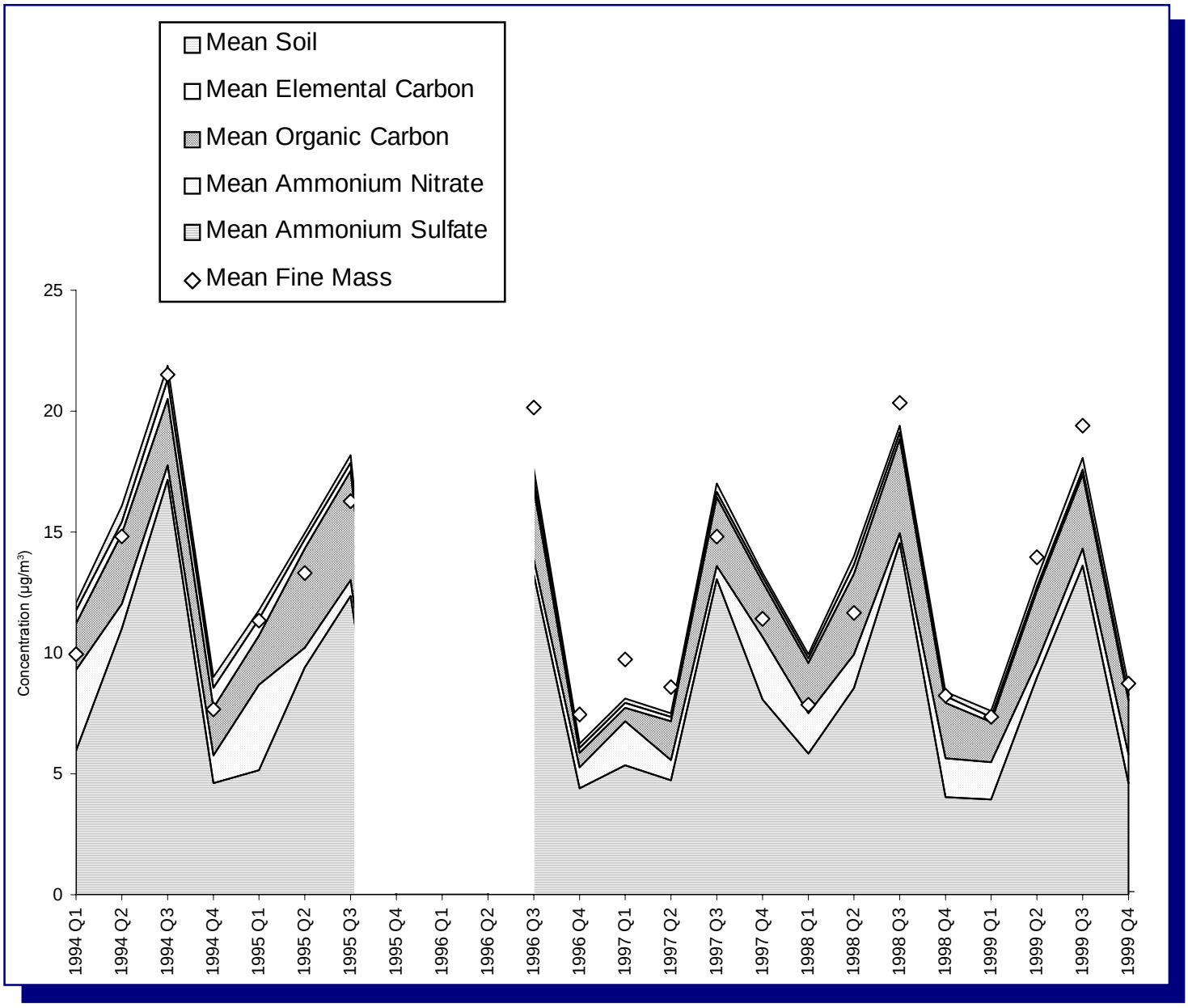

Figure 5-11. Time Series of Quarterly Reconstructed Fine Mass at Site LIV573

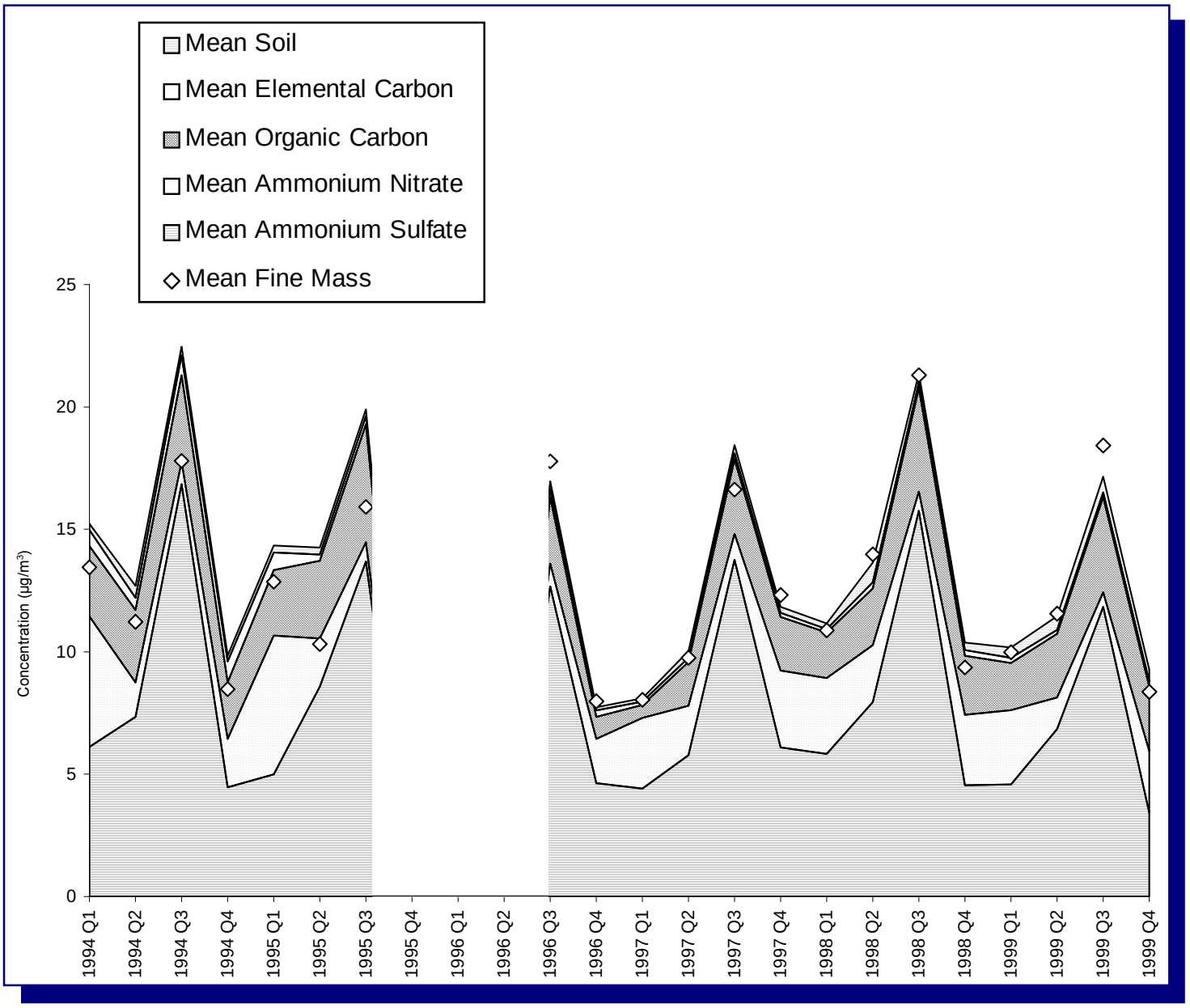

Figure 5-12. Time Series of Quarterly Reconstructed Fine Mass at Site BVL530

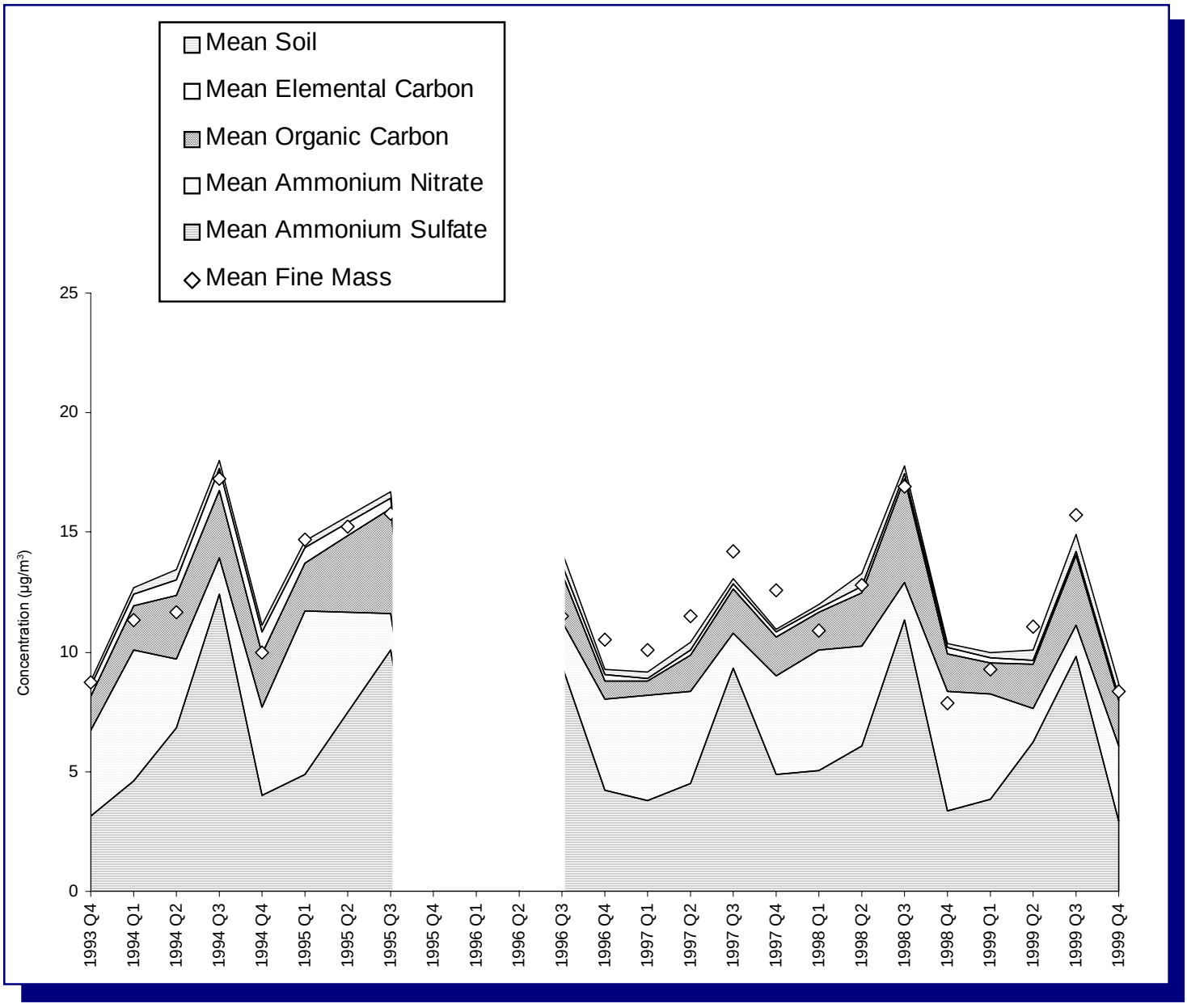

Figure 5-13. Time Series of Quarterly Reconstructed Fine Mass at Site CDZ571

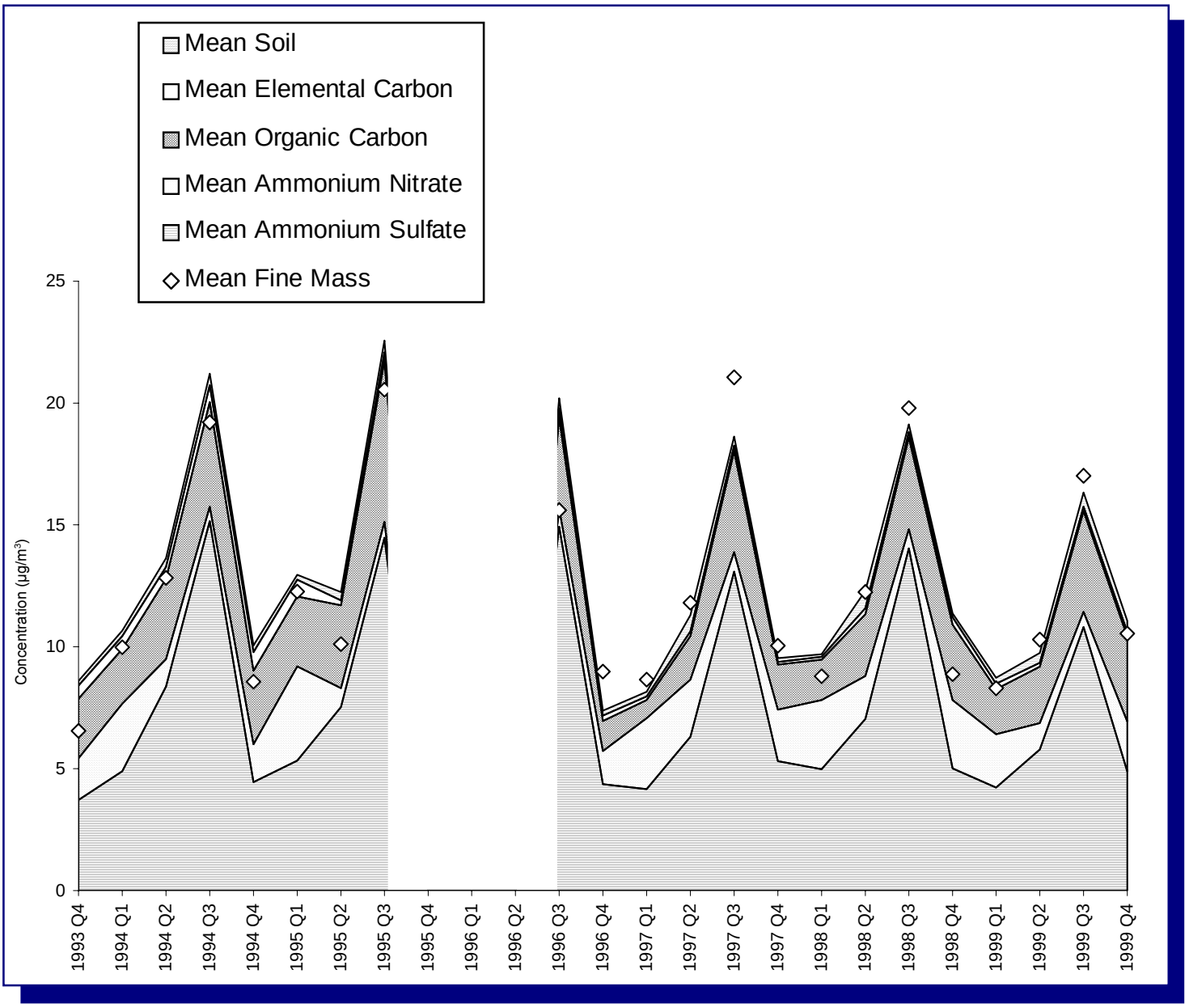

Figure 5-14. Time Series of Quarterly Reconstructed Fine Mass at Site SIK570

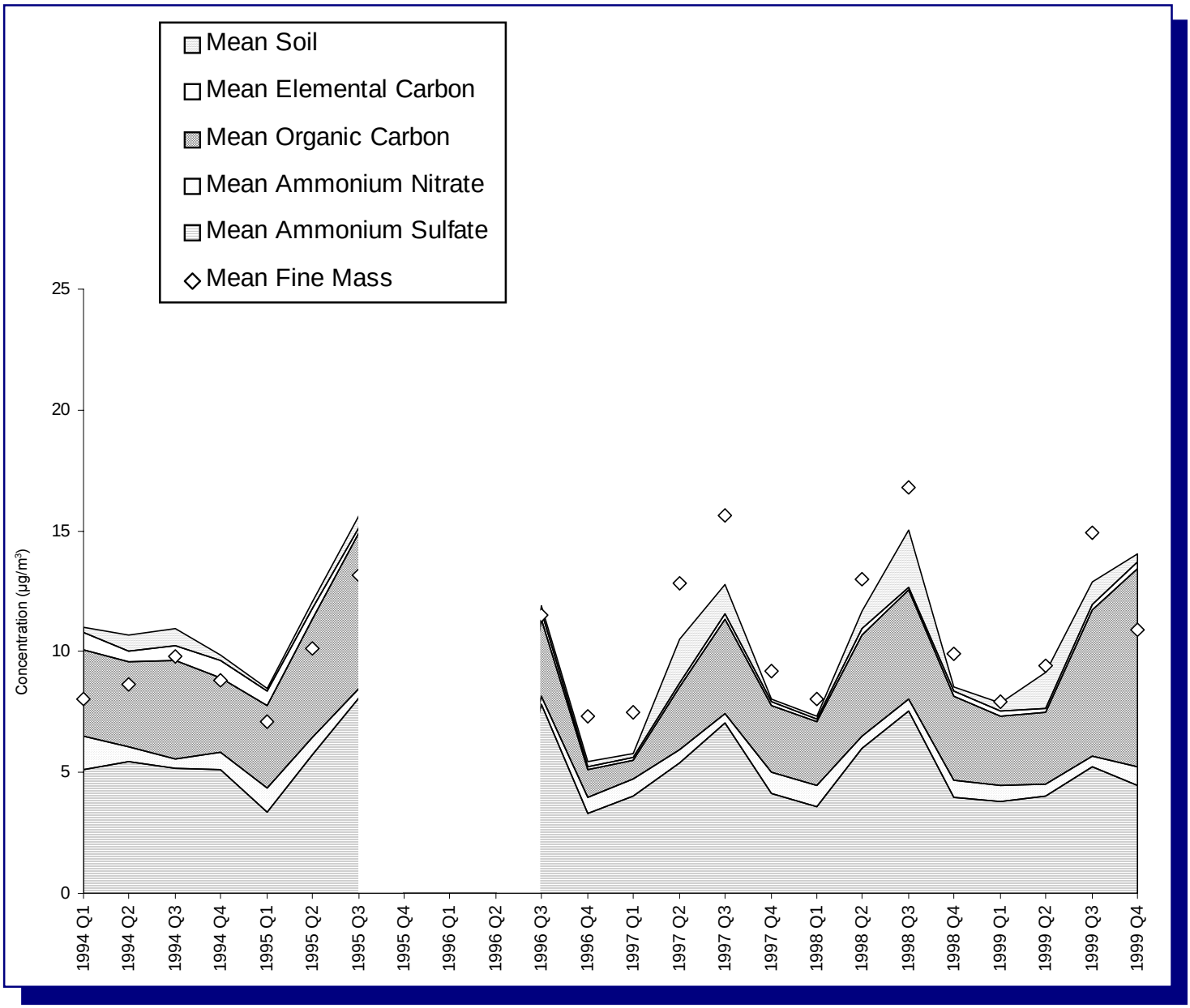

Figure 5-15. Annual and Peak 24-hour Fine Mass Concentrations and Chemical Constituents for Site CTH510

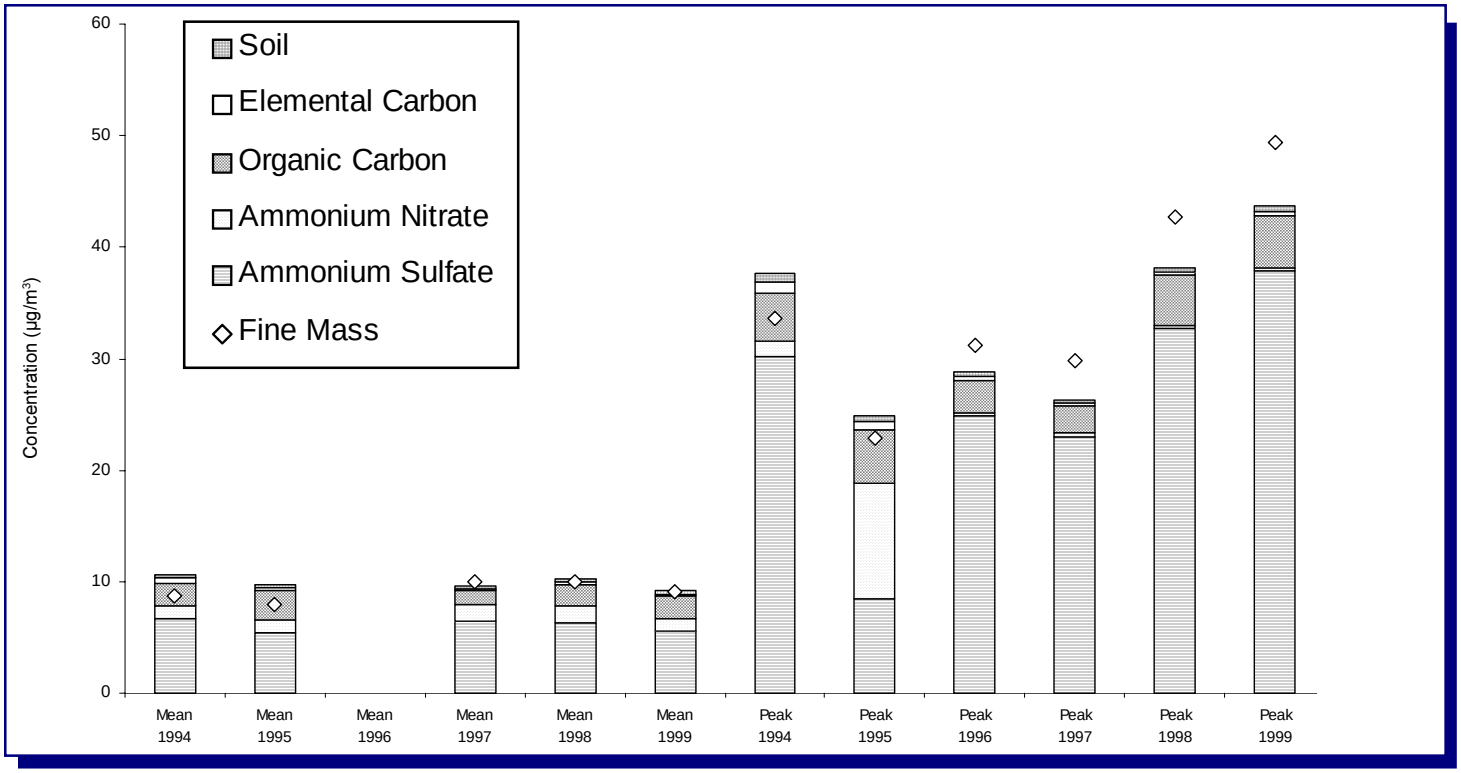

Figure 5-16. Annual and Peak 24-hour Fine Mass Concentrations and Chemical Constituents for Site ARE528

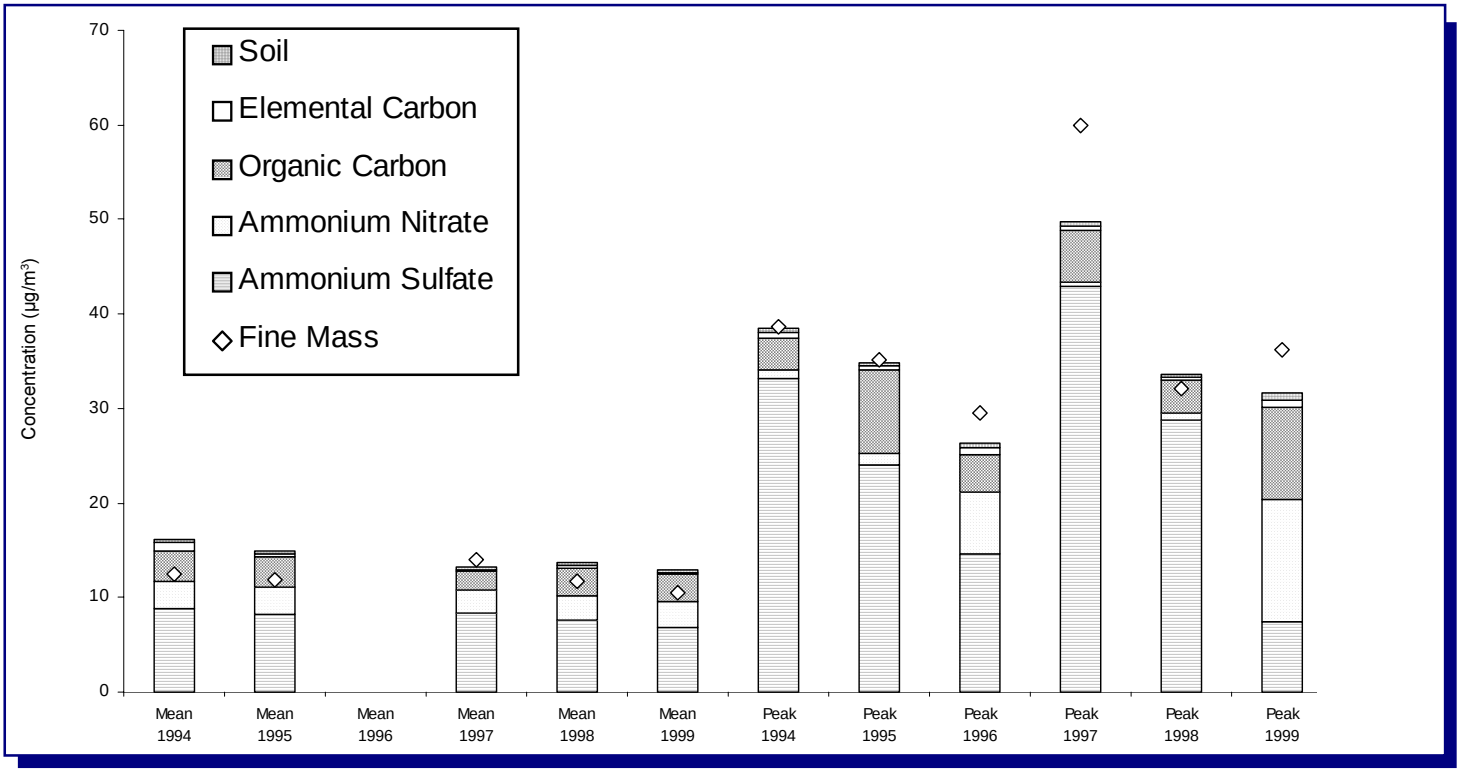

Figure 5-17. Annual and Peak 24-hour Fine Mass Concentrations and Chemical Constituents for Site MKG513

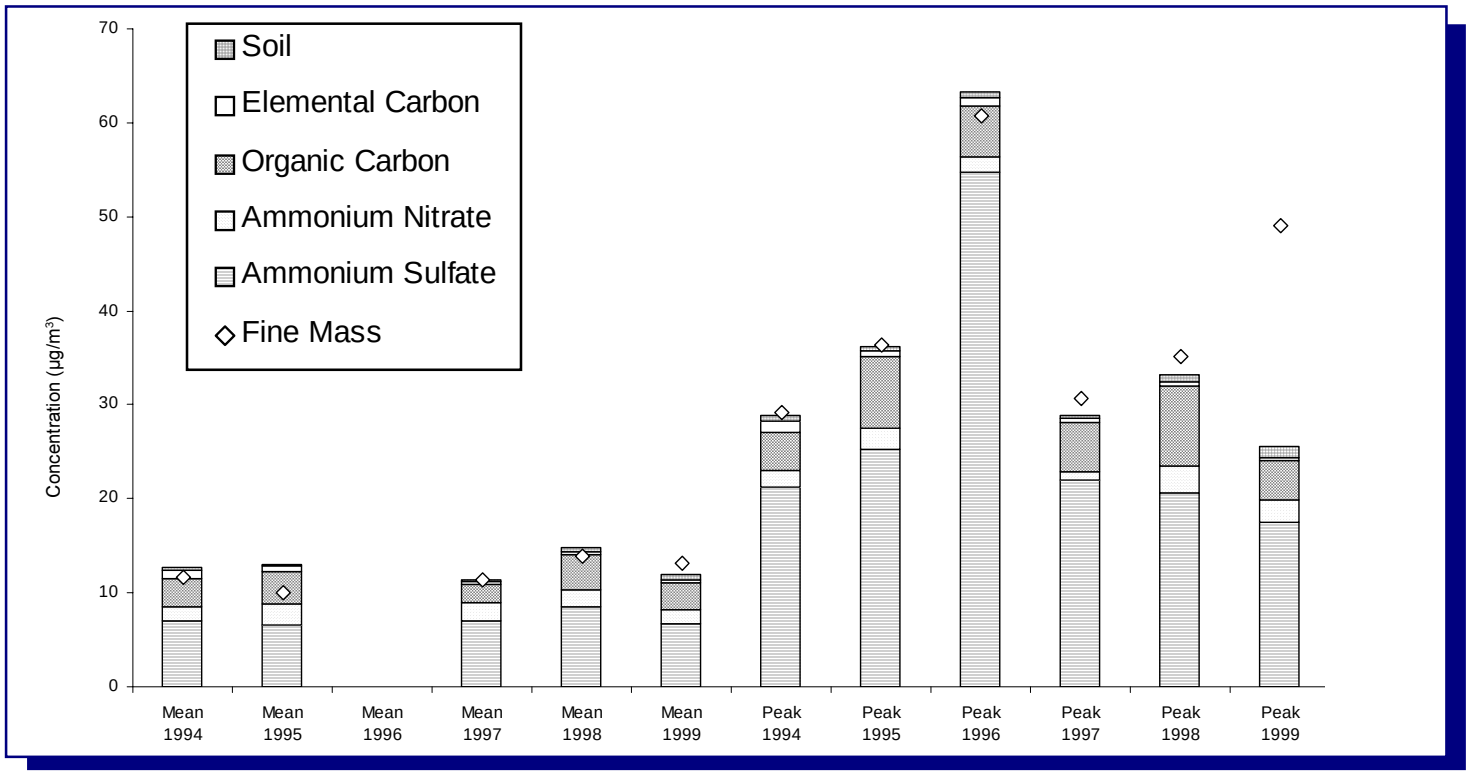

Figure 5-18. Annual and Peak 24-hour Fine Mass Concentrations and Chemical Constituents for Site QAK572

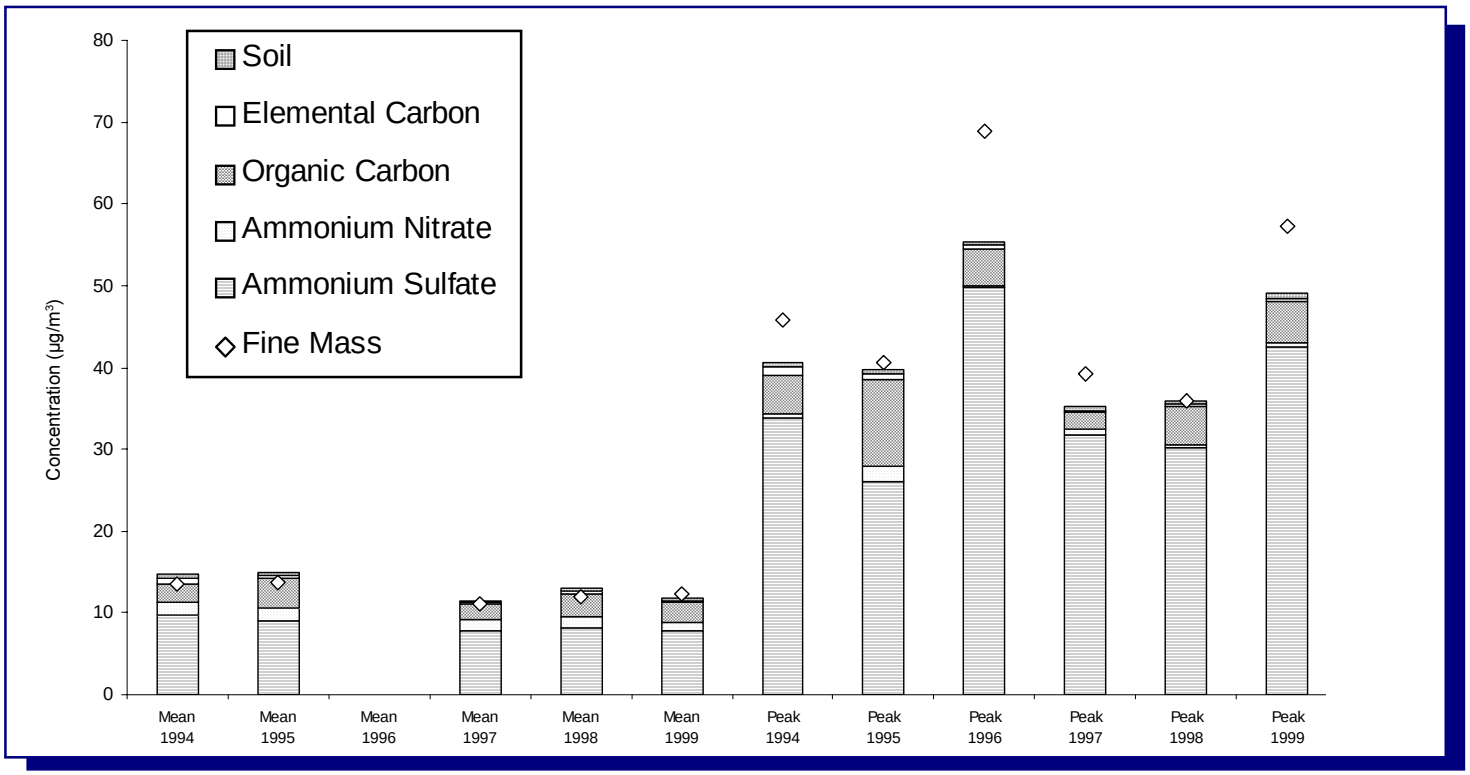

Figure 5-19. Annual and Peak 24-hour Fine Mass Concentrations and Chemical Constituents for Site LIV573

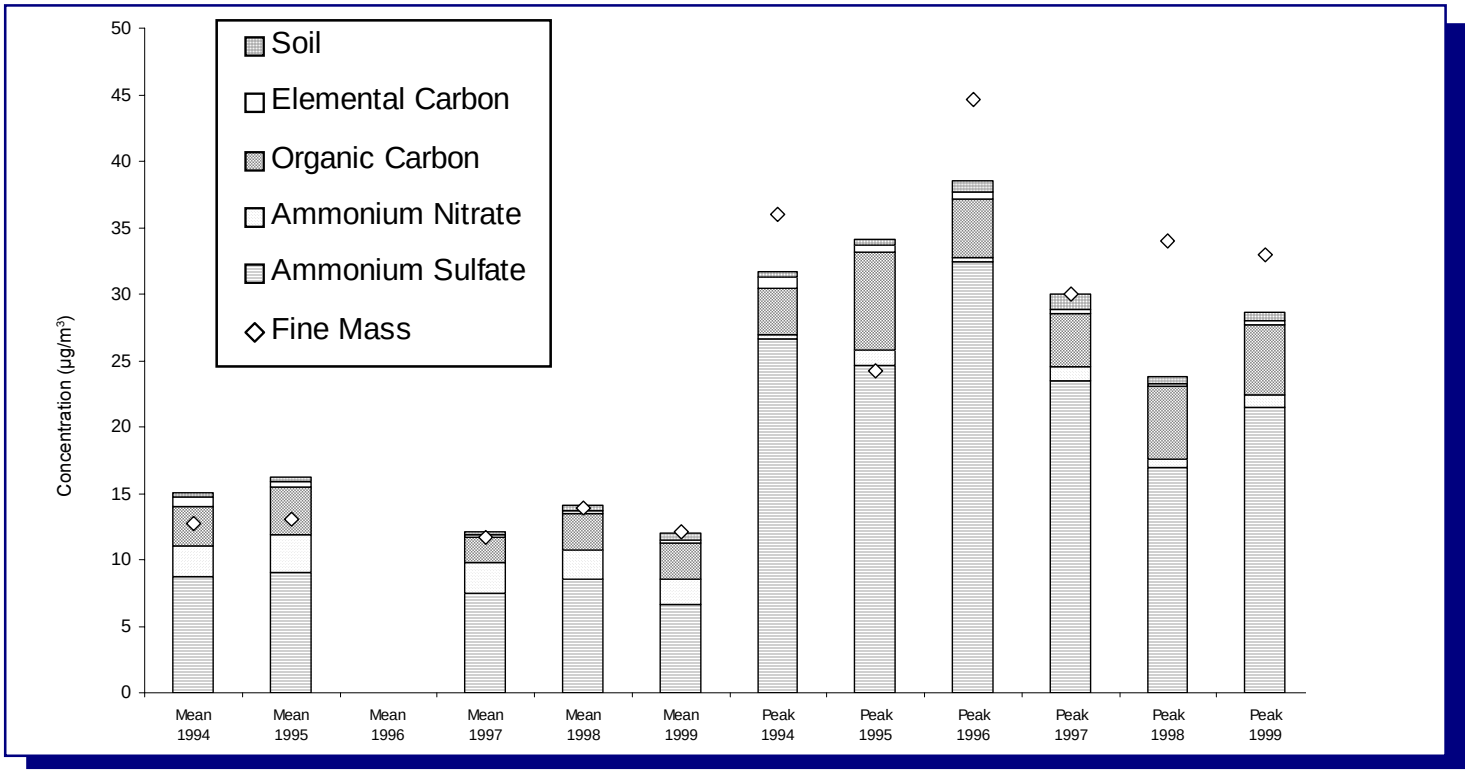

Figure 5-20. Annual and Peak 24-hour Fine Mass Concentrations and Chemical Constituents for Site BVL530

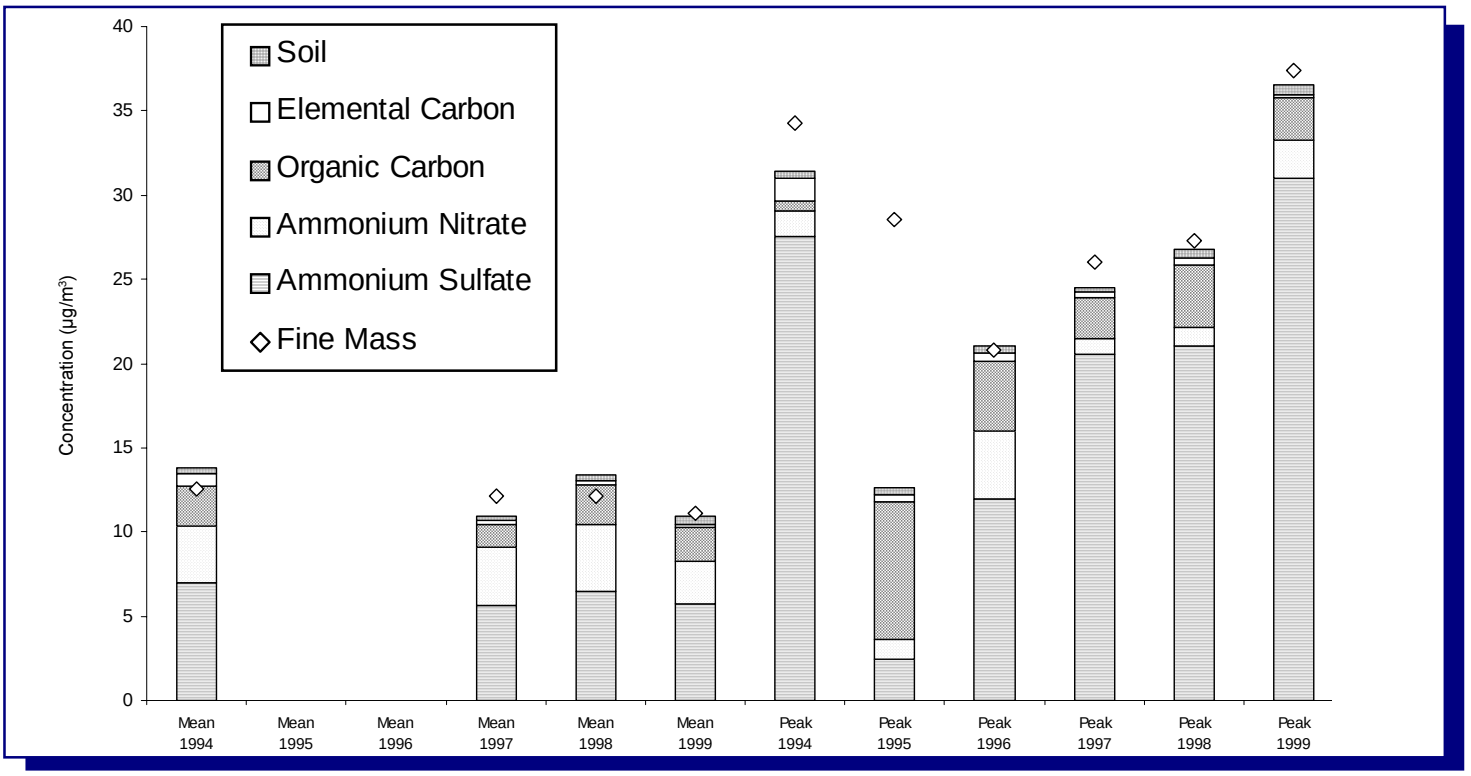

Figure 5-21. Annual and Peak 24-hour Fine Mass Concentrations and Chemical Constituents for Site CDZ571

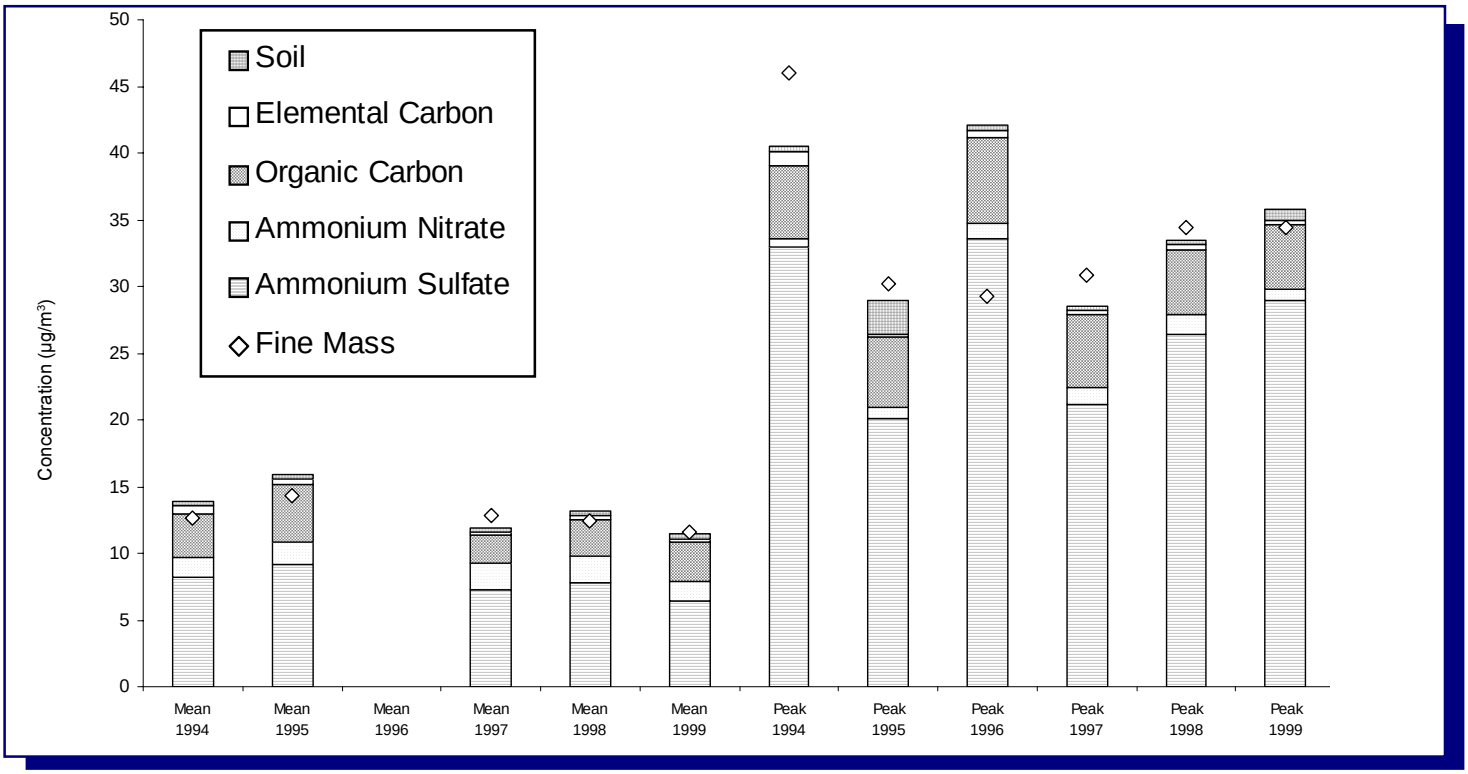

Figure 5-22. Annual and Peak 24-hour Fine Mass Concentrations and Chemical Constituents for Site SIK570

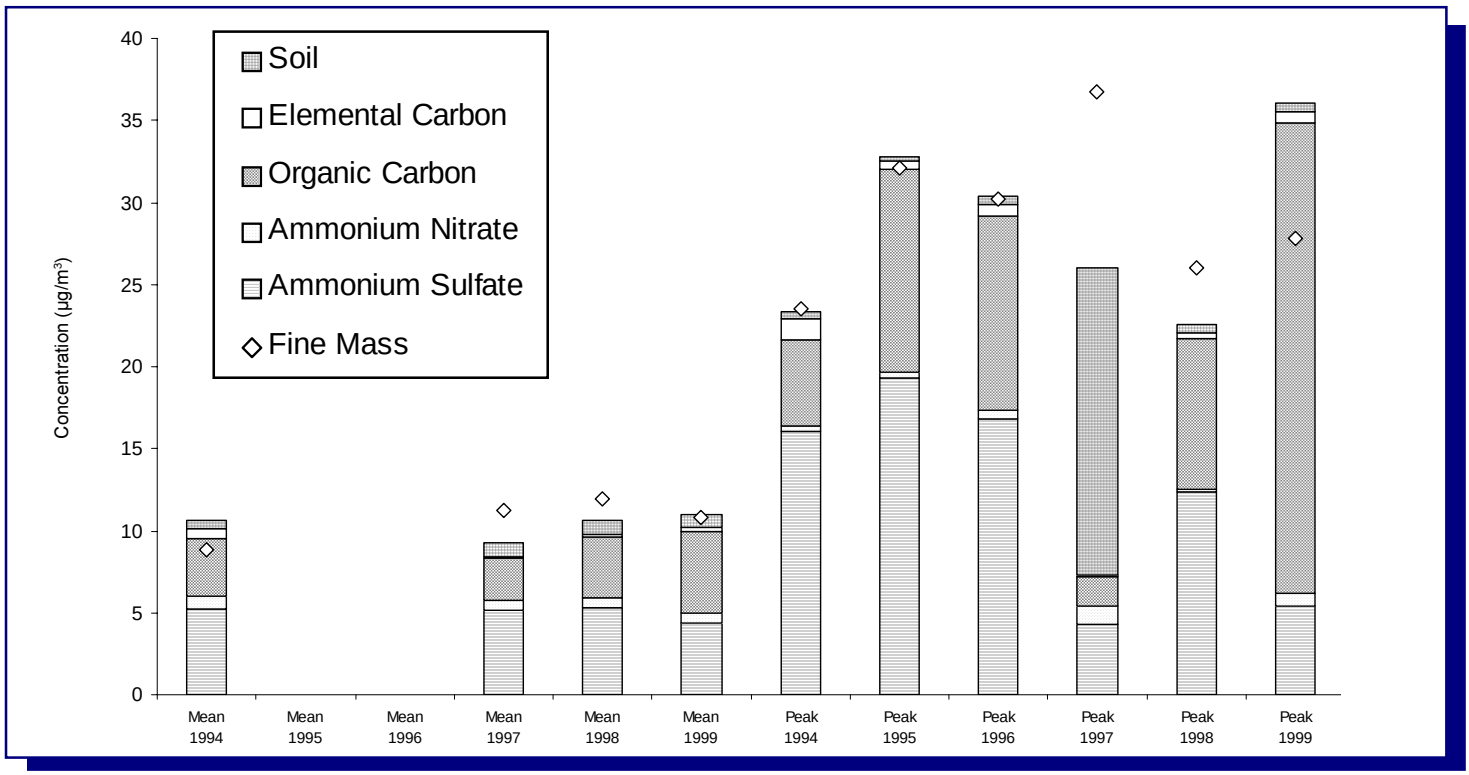

Figure 5-23. Trends in Annual Averages

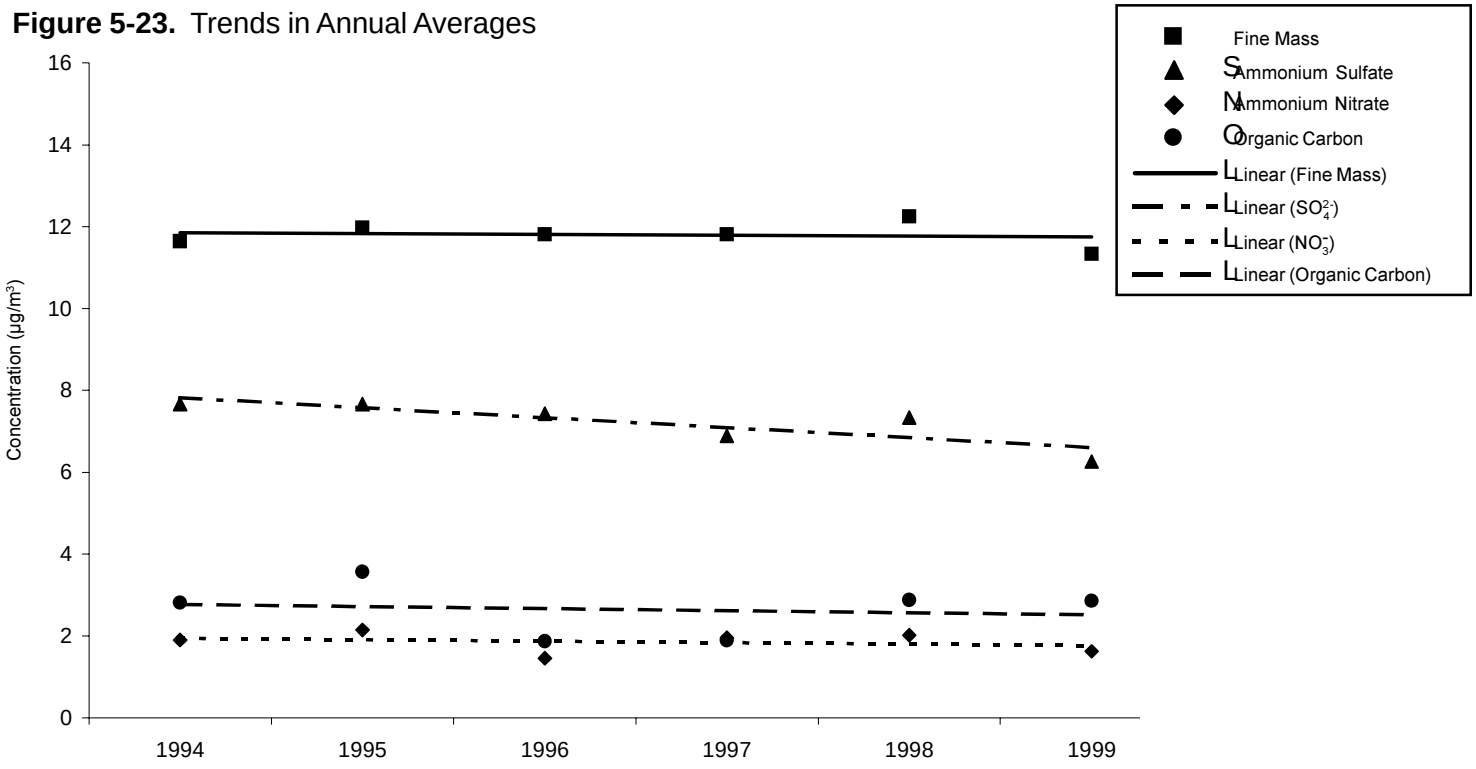

This page intentionally left blank.

Figure 5-24. Annual Average Trends in Composite Fine Mass

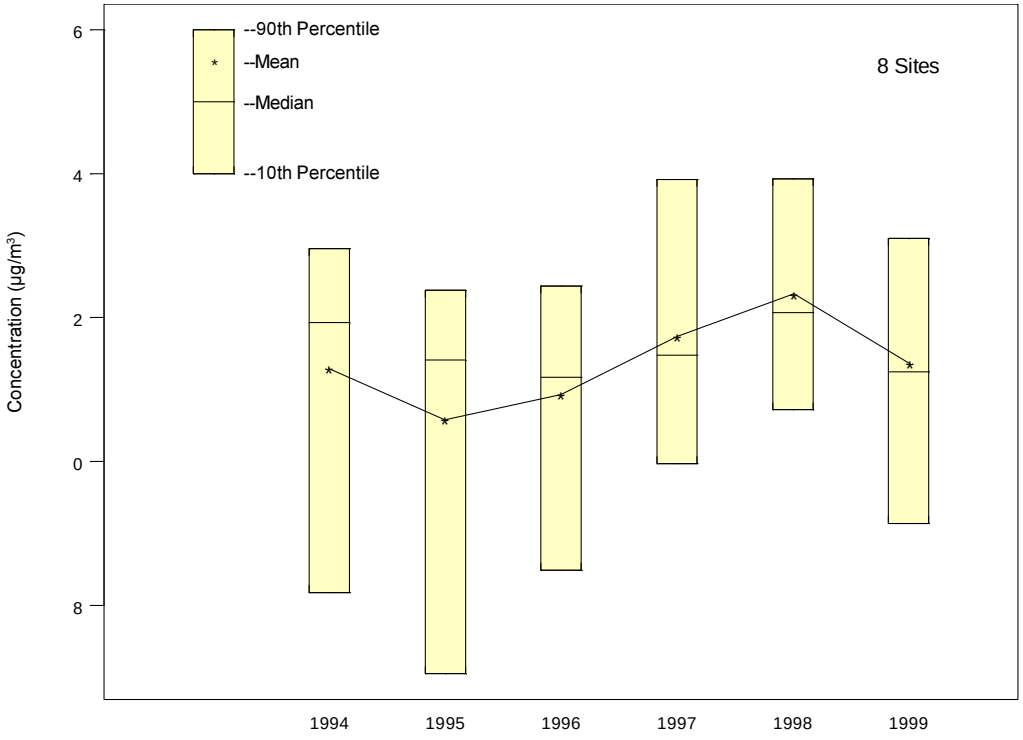

Figure 5-25. Annual Average Trends in Composite Ammonium Sulfate

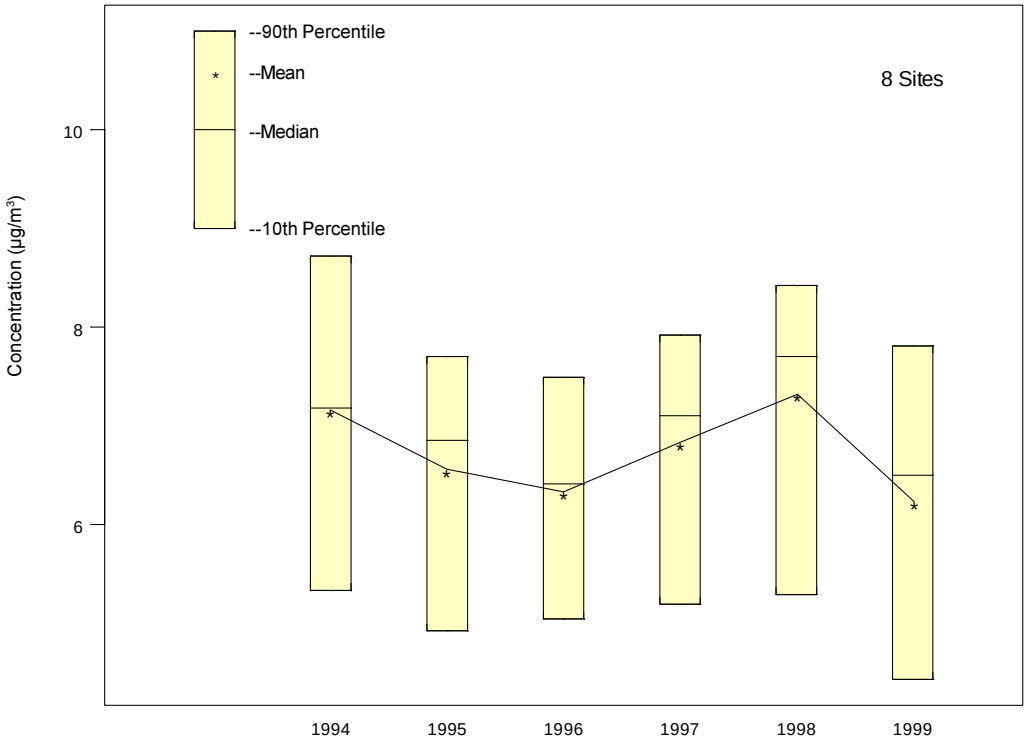

Figure 5-26. Annual Average Trends in Composite Ammonium Nitrate

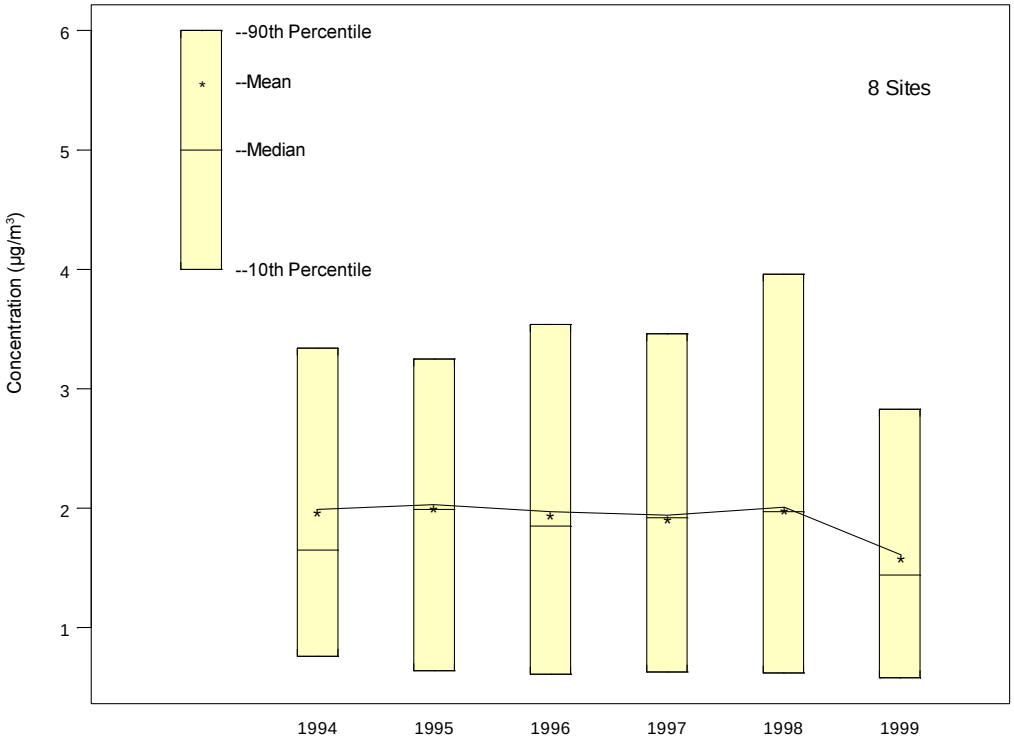

Figure 5-27. Annual Average Trends in Composite Organic Carbon

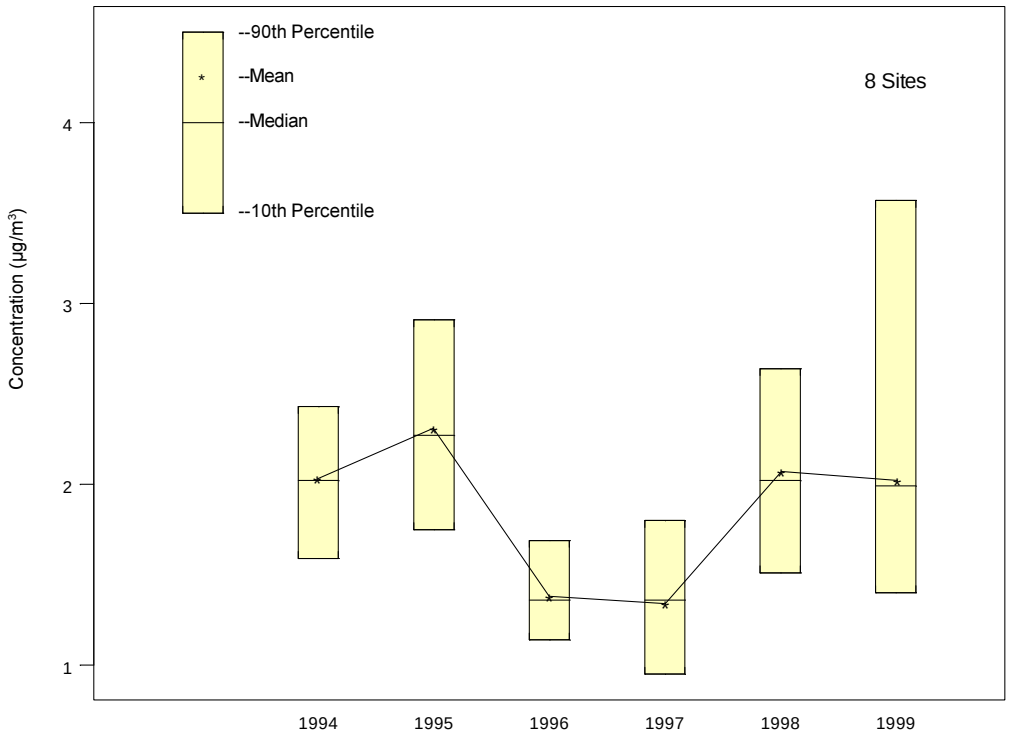

Figure 5-28(a). First and Second Quarter 1999 Scattergrams of 24-hour Fine Mass and SO_4^{2-} Concentrations for all Visibility Monitoring Sites

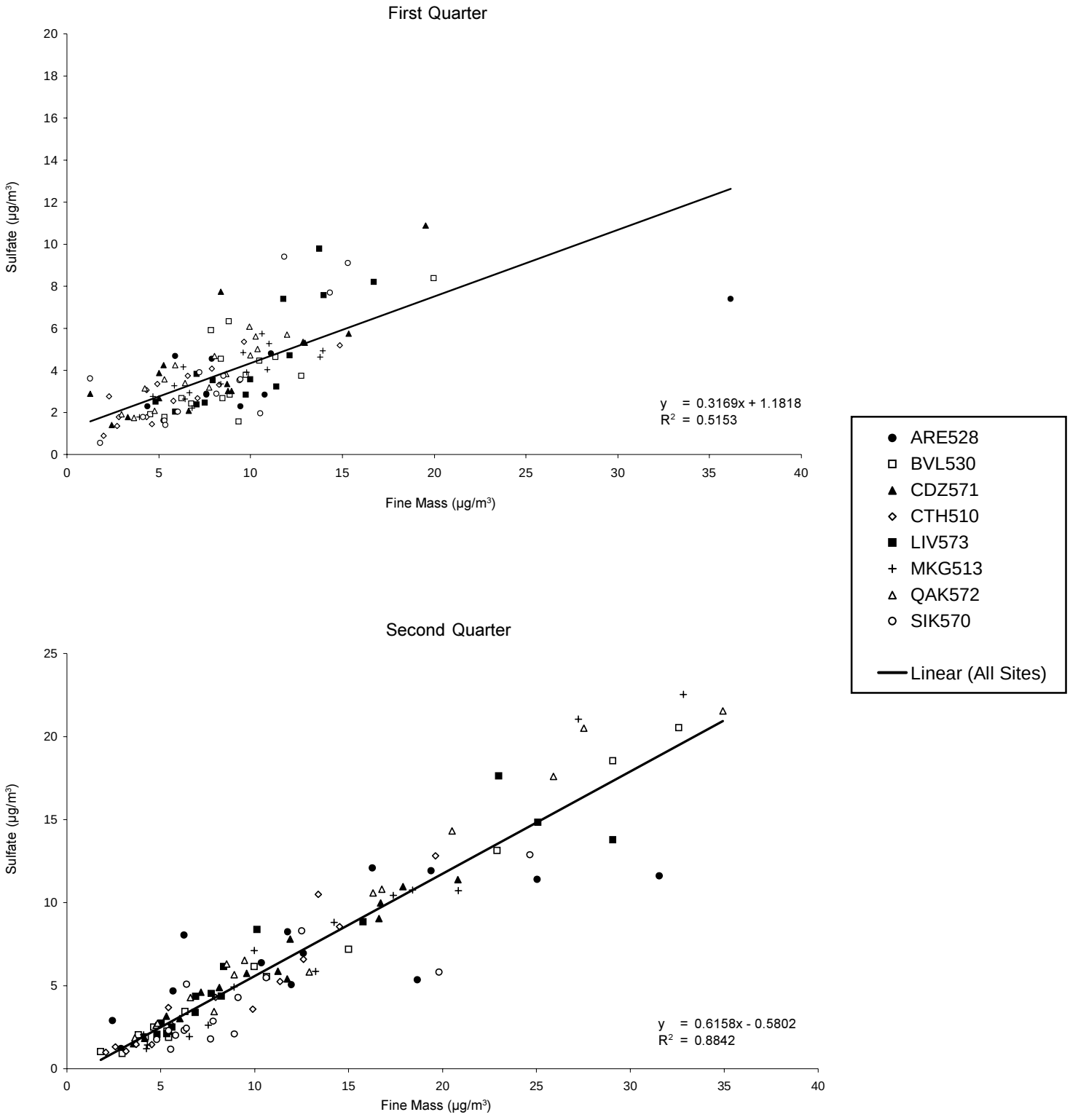

Figure 5-28(b). Third and Fourth Quarter 1999 Scattergrams of 24-hour Fine Mass and SO_4^{2-} Concentrations for all Visibility Monitoring Sites

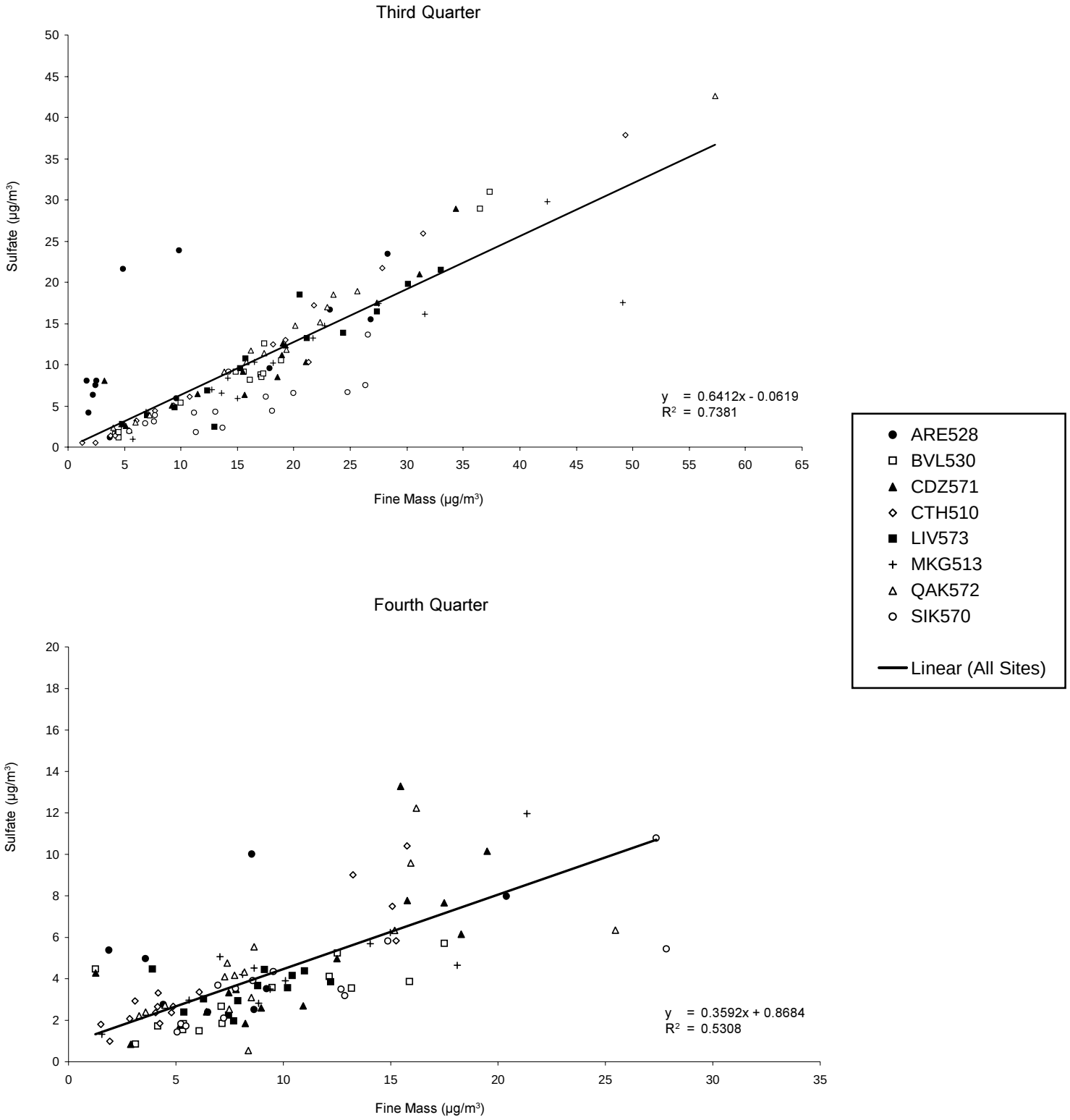

Table 5-1. Peak Annual Concentrations (µg/m^3) of Fine Mass and Its Chemical Constituents (1994 - 1999)

Site	$PM_{2.5}$ Mass	SO_4^{2-}	NO_3^-	Organic Carbon	Elemental Carbon	Soil
Connecticut Hill, NY	10.0	6.4	1.5	1.3	0.2	0.2
Arendtsville, PA	14.0	8.3	2.4	2.0	0.2	0.2
M.K. Goddard, PA	13.9	8.5	1.9	3.7	0.4	0.5
Quaker City, OH	13.6	9.0	1.7	3.5	0.5	0.3
Bondville, IL	12.6	7.0	3.4	2.4	0.7	0.3
Livonia, IN	13.9	8.5	2.3	2.7	0.2	0.4
Cadiz, KY	14.3	9.1	1.8	4.3	0.4	0.3
Sikes, LA	11.9	5.3	0.6	3.7	0.2	0.8

Table 5-2. Peak 24-Hour Concentrations (µg/m^3) of Fine Mass and Its Chemical Constituents (1994 - 1999)

Site	$PM_{2.5}$ Mass	SO_4^{2-}	NO_3^-	Organic Carbon	Elemental Carbon	Soil
Connecticut Hill, NY	49.4	37.9	0.3	4.6	0.3	0.5
Arendtsville, PA	60.0	42.9	0.4	5.6	0.3	0.6
M.K. Goddard, PA	60.7	54.7	1.6	5.5	0.8	0.7
Quaker City, OH	68.9	49.7	0.2	4.6	0.6	0.4
Bondville, IL	37.4	31.0	2.3	2.5	0.2	0.6
Livonia, IN	44.6	32.4	0.3	4.5	0.5	0.8
Cadiz, KY	46.0	33.0	0.6	5.5	1.1	0.3
Sikes, LA	36.7	4.3	1.1	1.8	0.1	18.7